

Monte Carlo Simulations for Gamma Measurements in Monitoring and Emergency Situations



Reference:

Dowdall M., Selnæs Ø.G. Monte Carlo Simulations for Gamma Measurements in Monitoring and Emergency Situations. StrålevernRapport 2006:9. Østerås: Norwegian Radiation Protection Authority, 2006.

Key words:

Monte Carlo, Calibration, Gamma Detectors, Measurement

Abstract:

The changing security situation with respect to threats posed by radioactive materials necessitates a degree of flexibility with respect to the ability to measure radioactive isotopes in a wide variety of environments. This report details the application of Monte Carlo based techniques to the widely used technique of gamma-ray spectrometry for both monitoring and emergency response measurements. The techniques are introduced, applied to a gamma detection system and the results analysed with respect to a number of relevant parameters.

Referanse:

Dowdall M., Selnæs Ø.G. Monte Carlo Simulations for Gamma Measurements in Monitoring and Emergency Situations. StrålevernRapport 2006:9. Østerås: Norwegian Radiation Protection Authority, 2006.

Emneord:

Monte Carlo, Kalibrering, Gamma Detektor, Måling

Resymé:

Stadige endringer i trusselbildet hva angår radioaktivt materiale gjør det nødvendig å ha en viss fleksibilitet når det gjelder muligheten til å analysere radioaktive isotoper i et vidt spekter i miljøet. Denne rapporten tar for seg bruk av Monte Carlo-baserte teknikker som kan anvendes i gammaspektroskopi både for overvåking og for beredskapsmålinger. Teknikkene er beskrevet og anvendt på et gamma-system, resultatene er presentert med hensyn til en rekke relevante parametre.

Head of project: Tone Bergan.

Approved:



Per Strand, Director, Department for Emergency Preparedness and Environmental Radioactivity.

46 pages.

Published 2006-08-01.

Printed number 100 (06-08).

Cover design: LoboMedia AS.

Printed by LoboMedia AS.

Orders to:

Norwegian Radiation Protection Authority, P.O. Box 55, N-1332 Østerås, Norway.

Telephone +47 67 16 25 00, fax + 47 67 14 74 07.

www.nrpa.no

ISSN 0804-4910

Monte Carlo Simulations for Gamma Measurements in Monitoring and Emergency Situations

Mark Dowdall
Øyvind G. Selnæs

Statens strålevern
Norwegian Radiation
Protection Authority
Østerås, 2006

Forord

Gammaspektroskopi utgjør den mest brukte radioanalytiske metoden for både miljøovervåking og for beredskapsmålinger. Analytiske teknikker som anvender denne metoden har i mange år basert seg på laboratorieprosedyrer der enkelte trinn kan være relativt dyre og tidkrevende å utføre. Beredskapsmessig ser man behov for et mer fleksibelt og tilpasset system enn det som brukes under normale forhold i laboratorier. Matematiske teknikker som er basert på Monte Carlo gir betydelige fordeler når det gjelder overvåking og beredskap. Modellering av detektoren og dens gamma-respons gjør det mulig å gjennomføre prosedyrer som eliminerer eller demper en mengde problemer som er assosiert med gammaspektroskopi og dens anvendelse i flere situasjoner. Slike prosedyrer kreerer også en viss fleksibilitet til gammaspektroskopi som kan forsterke dens effektivitet under radiologiske nødsituasjoner som har oppstått etter 2001. Denne rapporten introduserer selve konseptet rundt og demonstrerer anvendelsen av Monte Carlo-teknikker for gammaspektroskopi. Fordeler og ulemper med tidligere metoder diskuteres, og hvordan gammaspektroskopi kan bli forsterket som en radioanalytisk teknikk for både overvåking og beredskap.

Foreword

Gamma ray spectrometry constitutes the most often used radioanalytical technique for both environmental monitoring and emergency response measurements. Analytical techniques utilising the method have for many years been based upon laboratory based procedures, some stages of the techniques being relatively expensive and time-consuming to conduct. Emergency response requires a degree of flexibility and adaptability that has not generally been provided for by laboratory based methods. Mathematical techniques based on Monte Carlo procedures offer significant advantages with respect to both monitoring and emergency response. Modelling of the detector and its response to gamma ray photons allows for procedures to be conducted that eliminate or mitigate a wide range of difficulties associated with gamma ray spectrometry and its application to different situations. Such procedures also confer a degree of flexibility to gamma ray spectrometric measurements that may enhance its effectiveness in the sort radiological emergency situations that have been emergent since 2001. This report introduces the concepts involved and demonstrates the application of Monte Carlo techniques to gamma ray spectrometry, discussing the advantages and disadvantages of previous methodologies and how gamma ray spectrometry can be enhanced as a radioanalytical technique both for monitoring and emergency response.

Contents

1	Introduction	1
1.1	Gamma- ray Analysis with HPGe Detectors: Basic Principles	2
1.2	Configurations of HPGe Detectors	5
1.3	HPGe Detector Efficiency	6
1.4	Determination of Detector Efficiency	7
	<i>1.4.1 Considerations for the Empirical Determination of HPGe Detector Efficiencies</i>	7
	<i>1.4.2 Sample Distance, Geometry, Density and Composition</i>	7
	<i>1.4.3 True Coincidence Summation</i>	9
	<i>1.4.4 Curve Fitting</i>	10
	<i>1.4.5 Selection of Isotopes</i>	12
1.5	Current Procedures for Calibration of HPGe Detectors	12
	<i>1.5.1 Preparation of Standards</i>	12
	<i>1.5.2 Counting of Standards</i>	14
	<i>1.5.3 Calculation of Efficiency</i>	14
1.6	Discussion	15
2	Mathematical Calibration Methods	17
2.1	Monte Carlo Methods	17
	<i>2.1.1 Monte Carlo Codes</i>	20
2.2	VGSL (Virtual Gamma Spectroscopy Laboratory)	21
3	Experimental	22
	3.1 The Detector	22
	3.2 Characterisation of the Detector	22
	3.3 Shielding	23
	3.4 Point Source Measurements	23
	3.5 Simulation of Volumetric Sources	24
	3.6 Calculation of Efficiency Transfer Factors without Detector Characterisation	25
	3.7. <i>A priori</i> Determination of Total Coincidence Summation and Matrix Correction Factors.'	25
4	Results and Discussion	27
	4.1 Modelling of Detector Efficiencies	27
	4.2 Efficiency Transfer	33

4.3 Density- Matrix Correction Factors	35
4.4 Spectral Simulation	36
4.5 Total Coincidence Summation Correction	40
4.6 Implementation in Analysis Systems	41
5 Conclusions	43
Acknowledgements	43
References	44

1. Introduction

The ability to make accurate and precise quantitative and qualitative assays of radioactive materials has long been a primary objective in a wide variety of scientific fields. For a number of reasons, a significant proportion of the effort has been devoted to laboratory based measurement techniques and the development of methods and procedures that allow for good quality measurements to be performed within the laboratory environment. These methods have to date often implemented procedures that are by necessity relatively time consuming and inflexible. Changing requirements within the fields where measurements of radioactive materials are made have necessitated the consideration of the suitability of currently commonplace laboratory based procedures for the new challenges in the area of radiation measurement. One of the primary concerns in this context is the ability to make accurate measurements of potentially complex samples, with respect to both the contaminants present and the nature of the samples upon which the measurements are made, in a relatively fast and flexible way in situations that may be outside of the normal laboratory environment and its support facilities.

The field of emergency preparedness with respect to radioactive materials and situations where the public may be exposed to radioactive materials in the 21st century presents a suite of challenges of some pertinence to the authorities responsible for producing accurate measurements of radioactivity. The changing nature of the risks and threats associated with radioactive materials necessitates an increase in the degree of flexibility in measurement methods and the recognition that such measurements may have to be made in environments far removed from the laboratory and on samples and materials that may not normally fall within the suite of samples analysed in the laboratory

within a time frame that is considerably less than usually available for more conventional measurement methods.

The advent of high purity germanium (HPGe) and silicon (Si) detectors during the course of the 1960's revolutionised the field of gamma ray spectrometry and such detectors remain the mainstay of the majority of radioanalytical laboratories around the world. The non-destructive nature of the technique, the generally high resolving power of the detectors and the potential for relatively automated analyses has meant that gamma-ray spectrometry using semiconductor detectors has enjoyed predominance in the field of radioanalytical science, be it for emergency response, applied physics, environmental radiochemistry or a host of other applications. The use of such detectors to produce accurate and precise results is in the main reliant on the establishment of the instruments ability to detect gamma radiation incident on the detector at various energies. This determination of what is commonly known as the detectors' efficiency may appear straightforward on first consideration yet it remains one of the more difficult operations for a number of reasons. As all subsequent results produced by a detector are to a large extent dependant on this efficiency calibration, some effort, thought and time must be expended on how the detector will be calibrated, what factors may have an effect on the validity of the produced calibration and how such factors may be compensated for or their effects mitigated.

The traditional approach to the efficiency calibration of semi-conductor gamma-ray detectors is to directly determine the detectors response to gamma radiation of various energies by exposing the detector to known activities of selected specific isotopes. The efficiencies calculated for the chosen isotopes/energies are then extrapolated across the desired energy range of interest to produce an efficiency curve.

The efficiency values provided by this curve are then used to calculate the activities of isotopes present in samples whose gamma-ray emissions may not have been included in the suite of gamma-rays used to produce the original curve. Although this approach is almost ubiquitous in practice and initially appears quite straightforward, the process includes a number of pitfalls and considerations that must be made to ensure accurate and precise results. Of some concern also is the time and expense required to conduct such empirical calibrations, limitations imposed by the procedure regarding sample sizes and matrices and the generation of waste radioactive materials. Because of these and other considerations, mathematical calibration of detectors has received attention in the past and the implementation of these techniques has been the focus of much research in recent years.

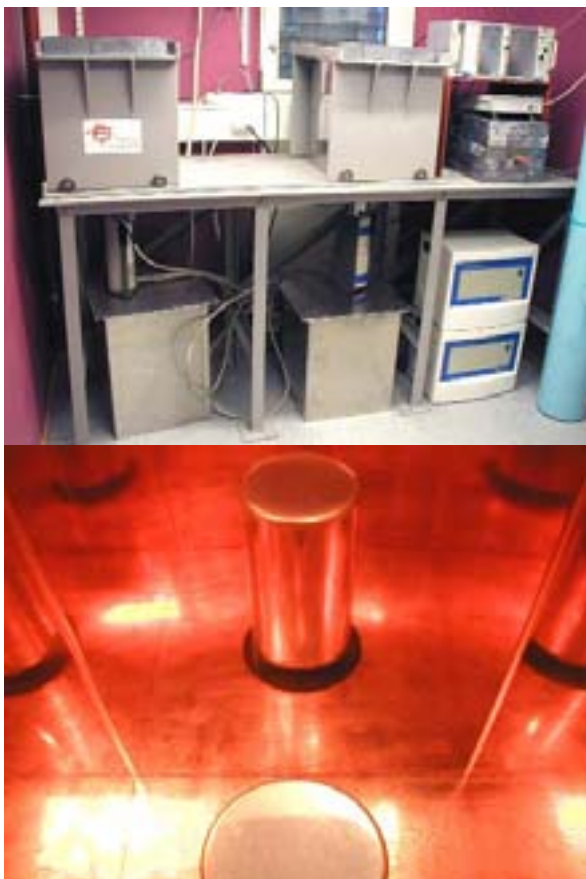


Figure 1.1 Two electrically cooled HPGe detectors and shielding at the laboratories of the NRPA, Tromsø (top), close up of an HPGe detector inside a copper/tin lined lead shield (bottom).

This report introduces the factors that affect the efficiency of HPGe detectors, typical methods of HPGe spectrometer efficiency calibration, briefly presents the problems to be overcome using these methods, the advantages and disadvantages of such methods and introduces possible alternative procedures using mathematical calibration procedures. The implementation of a mathematical calibration procedure is presented and its use with respect to the calibration of a typical HPGe detector is described and discussed.

1.1. Gamma-ray Analysis with HPGe Detectors: Basic Principles

High Purity Germanium detectors, commonly referred to as HPGe detectors, are based around the construction of p- or n- type semiconductor diodes from high purity germanium crystals. The manufacturing process is such that the diode can withstand cryogenic temperatures and high voltage, low current reverse biases. The Ge crystal has a p⁺ and an n⁺ contact (Fig. 1.2) formed by ion implantation or other techniques.

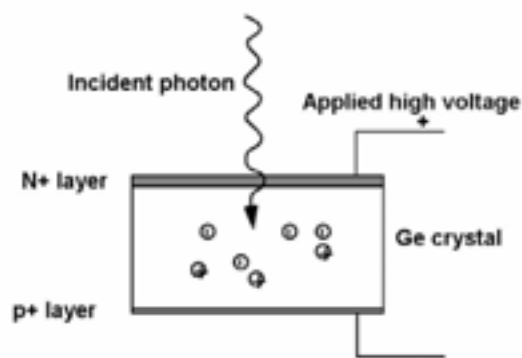


Figure 1.2. Schematic of HPGe semiconductor detector

When a high voltage is applied across the crystal, the depletion of charge carriers causes the formation of a depleted zone within the crystal (the “intrinsic zone”). Interaction of a gamma-ray photon with the intrinsic zone of the detector results in the release of electrons and

corresponding “electron holes” which move to the contact of opposite polarity along the electric field established by the applied high voltage. The charge produced by the interaction is integrated by a charge sensitive preamplifier and an electric

“bins” or channels, each of these channels corresponding to a specific voltage. As the digital pulses arrive in the MCA they are allotted to the appropriate channels. If a mono-energetic gamma-ray source is placed on a detector, then

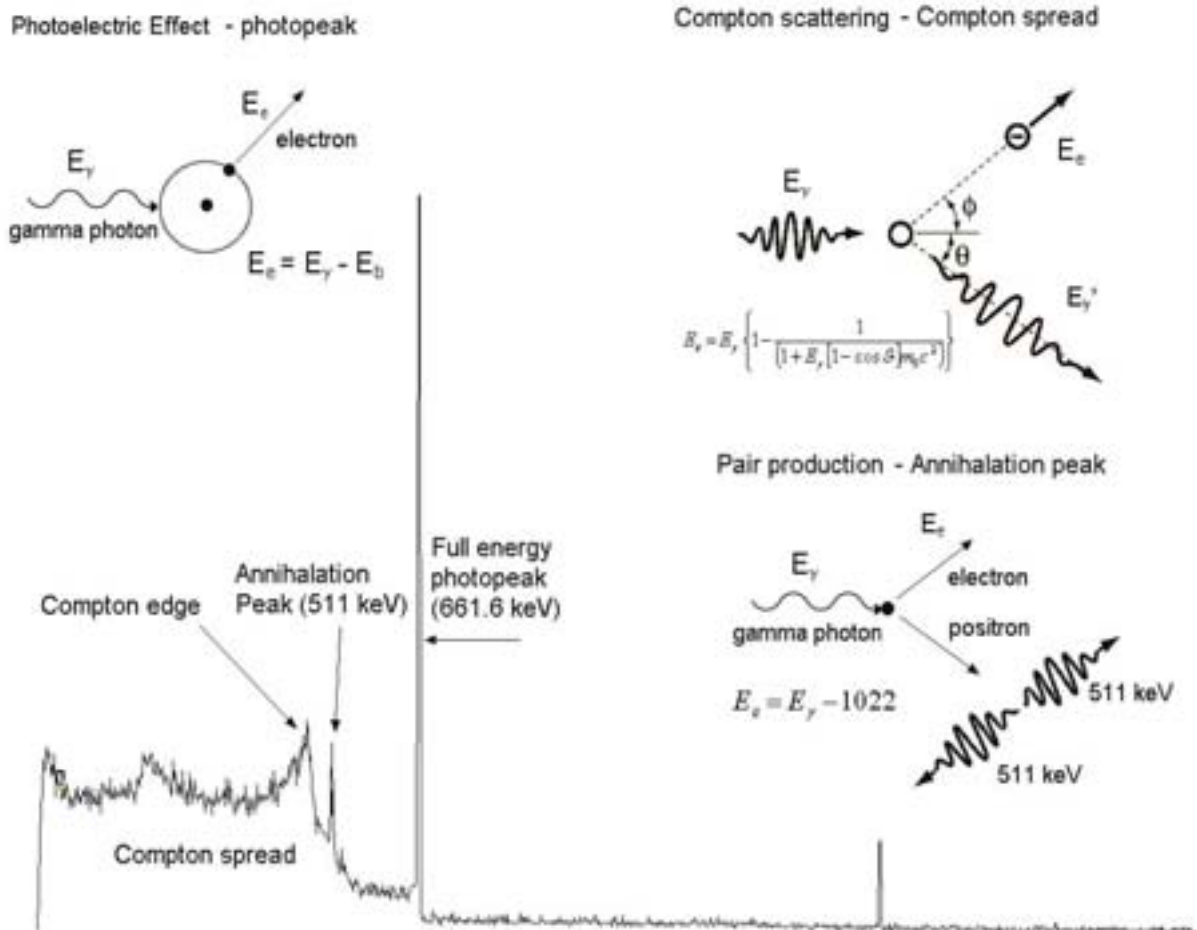


Figure 1.3. Typical HPGe gamma-ray spectrum (^{137}Cs) displaying the characteristic spectral features of the three dominant interaction processes of gamma-ray photons with the detector. It should be noted that the above spectrum is of a mono-energetic source; sources with multiple gamma-ray photons will display features due to Compton scattering and the photoelectric effect for all individual peaks.

pulse is produced, the voltage of which is directly proportional to the energy of the incident photon. This pulse is then passed along the signal processing chain within which the pulse is cleaned and shaped by an amplifier and then passed to an Analog to Digital converter (ADC). The pulse is ascribed a “number” according to its voltage and is then passed to a Multichannel Analyser (MCA). The MCA divides a given voltage range into a series of

more pulses corresponding to the energy of the emitted gamma-rays arrive at the MCA and the channels corresponding to that voltage receive more pulses (or “counts”) than the other channels and a peak is formed. On a simplistic level, if two gamma-rays of known energy are incident on the detector, then observing which channels contain the peaks allows the range of channels to be ascribed energies resulting in the energy calibration of the detector.

The situation is however complicated by the fact that a mono-energetic gamma-ray incident on the detector will not only produce pulses corresponding to that gamma-ray. Statistical fluctuations and electronic noise within the system will result in broadening of the peak which will now occur in a range of channels rather than just the one corresponding to the energy of the incident gamma-ray photon. Some electron-hole pairs do not reach the electric contacts of the detector and this results in tailing of the peak on the low energy side. Some photons will not deposit all their energy within the intrinsic region of the crystal and will undergo inelastic scattering and escape from the intrinsic region. Others will be scattered or absorbed by the shielding or materials used in the construction of the detector. Of some consequence also is the fact that the construction of HPGe detectors results in the formation of dead layers within the crystal at the n+ and p+ contacts with thicknesses of the order of 700 μm and 0.3 μm respectively. These dead layers tend to be of non-uniform thickness over the crystal and the transitions between the dead layer and the active crystal may also not be well defined. These areas act as absorbers due to the fact that they are not available for charge collection.

Irrespective of the above discussion, three primary processes are dominant when considering how gamma-ray photons interact with germanium detectors (Fig. 1.3.). The first, photoelectric absorption, occurs when the incoming gamma photon imparts, to all intents and purposes, all of its energy to an electron of an atom within the detector crystal. The process results in a count being deposited within the channels corresponding to the full energy photopeak of the gamma-ray spectrum. If the gamma-ray photon only imparts a portion of its energy to the electron due to striking it at an angle, the pulse produced will not represent the full energy of the incident gamma-ray. The distribution of energies imparted to the electron is a function of the angle of impact and can

range from an angle of 0 degrees where no energy is imparted within the detector crystal to an angle of 180 degrees. The resulting distribution of energies appears in the spectrum as a continuum below the full energy peak for a mono-energetic gamma-ray. The process producing this continuum is known as Compton scattering and hence the distribution is known as the Compton spread. Unlike the two processes mentioned previously, the third involves interaction with an atom as a whole rather than the interaction between the incident photon and an electron. This interaction results in the formation of an electron-positron pair. As this requires a photon with energy greater than the rest mass of the two particles (511 keV each), the process is only relevant for photons with energies greater than 1022 keV. Once formed, the positron will annihilate an electron resulting in the release of two 511 keV annihilation photons, the phenomenon manifesting itself within the spectrum as a peak at 511 keV. The dominance of these processes as a function of energy for a HPGe detector are displayed in Fig. 1.4. Space constraints confine the above discussion to a relatively simplistic level but further information may be found in any standard physics text or in Knoll (2000), Tsoulfanidis (1983) or Debertin and Helmer (1988).

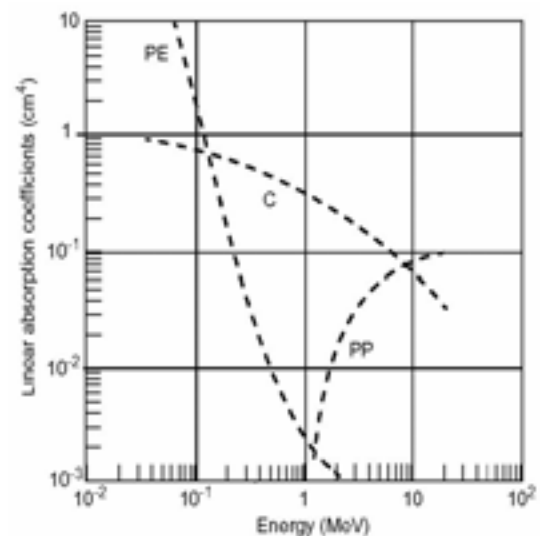


Figure 1.4. Linear absorption coefficients as a function of energy for a HPGe detector. Pe – Photoelectric absorption, C – Compton Scattering, PP – Pair Production.

1.2 Configurations of HPGe Detectors

The configuration of the detector, both with respect to the crystal shape and dimensions and the nature of the construction materials used to house the detector, has a significant effect on the efficiency. The standard HPGe detector is a coaxial p-type detector, the germanium crystal itself being typically some 60 mm long and of similar diameter in a cylindrical geometry. Manufacturers have however produced a variety of configurations in order to both extend the energy range over which HPGe detectors are useful and in order to maximise efficiency, resolution or both. The most conventional configuration for HPGe detectors is the p-type coaxial detector (Fig. 1.5.). The n and p contacts for such detectors are typically diffused lithium (approx. 0.5 mm thick) and implanted boron (approx. 0.3 mm thick) respectively. Such detectors offer an effective energy range between 40 keV and approximately 10 MeV although efficiency is low at the higher energy ranges.

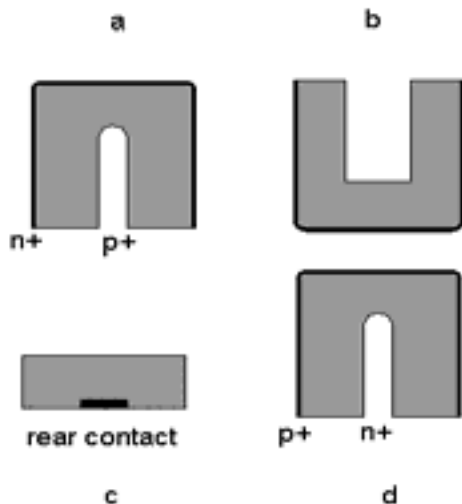


Figure 1.5. Representations of the most common HPGe detector configurations. *a* – standard HPGe p-type coaxial, *b* – HPGe well detector, *c* – planar HPGe, *d* – n-type HPGe.

HPGe detectors in a “well” configuration offer close to 4π configuration and therefore exhibit

high efficiencies (with concomitant summation problems) with some manufacturers claiming good response down to 10 keV. Planar configurations which may be n- or p- type, offer good responses to very low energies, many manufacturers claiming a range of 3 keV to 1 MeV for n-type and 0.2 keV to 1 MeV for p-type.

In addition to crystal size or geometry, the housing of the detector plays an important role in relation to the detectors efficiency and performance. The conventional mounting for a HPGe detector is to surround the crystal with a mounting cup (Fig. 1.6.) which may also form the outer contact with the detector. The thickness of this cup and the materials used in its construction affect efficiency via absorption of incoming photons.

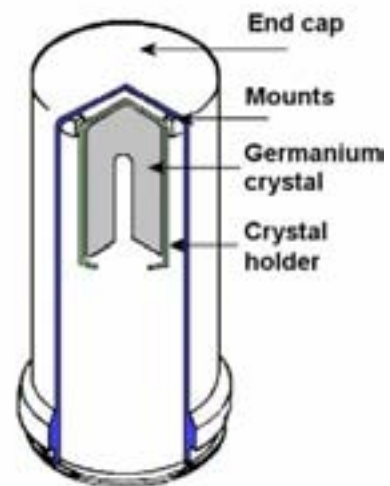


Figure 1.6. Schematic cutaway of a coaxial p-type HPGe indicating constructional features of pertinence regarding detector efficiency. Typical constructional materials for endcap, mounts and crystal holder include aluminium and copper.

The detector and its mounting cup are then placed in the “end cap” which is typically housing constructed of aluminium and which constitutes the visible part of the detector. There may also be mounting materials used to hold the

detector firmly within the endcap and at the correct orientation. The thickness of the endcap, its construction material and the distance between the detector face and the inner surface of the endcap all have a significant bearing on the efficiency of the detector. In an effort to reduce the effect of attenuation by the endcap, some detectors are produced with a window in the endcap, the window being of lesser thickness than the endcap material itself and often constructed of materials such as beryllium or various polymers of low Z numbers. These windows not only serve to reduce the lower energy limit for which the detector is effective but also to increase the efficiency of the detector at lower energies by reducing the attenuation of incoming photons.

The selection of detector configuration is obviously related to the application to which the detector will be put, certain configurations not being suitable for certain tasks. However the above serves to highlight the facets of the physical nature of detectors and their housing of pertinence to any discussion relating to detectors efficiency.

1.3. HPGe Detector Efficiency

Before considering the efficiency calibration of HPGe detectors it is worth introducing a number of definitions related to the concept of efficiency. Four different measures of detector efficiency are in common usage.

- 1) *Relative Efficiency*: a measure of the performance of a detector (usually denoted as ϵ_{rel}) relative to a standard 3x3 inch sodium iodide (NaI) scintillation detector, most often expressed for the 1332 keV gamma-ray of a ^{60}Co point source at 25.0 cm from the detector endcap. The efficiency for such an arrangement with an NaI detector is

typically 1.2×10^{-3} . The relative efficiency of an HPGe detector can easily be related to the volume of the detector or its dimensions by either of the following:

$$\epsilon_{rel} = V / 4.3 \quad [1]$$

where V is the detector volume in cm^3 ,

$$\epsilon_{rel} = kd^\alpha l^\beta \quad [2]$$

where $k=243.21$, $\alpha = 2.8155$, $\beta = 0.7785$ and d and l are diameter and length (dm) respectively.

- 2) *Absolute Full Energy Peak Efficiency*: a measure of the relationship between the net peak area of the energy of interest relative to the number of gamma-rays emitted by the source at that energy and usually denoted as ϵ_{peak} ;
- 3) *Absolute Total Efficiency*: a measure of the number of gamma-rays of any energy emitted by the source relative to the number of counts occurring in the spectrum as a whole including the full energy peak and all incomplete absorptions and usually denoted as ϵ_{tot} ;
- 4) *Intrinsic Efficiency*: a measure of the number of counts in the spectrum relative to the number of gamma-rays emitted by the source which are incident on the detector and may be expressed for either the full energy peak (Intrinsic Full Energy Peak Efficiency) or the total spectrum (Intrinsic Total Efficiency). Intrinsic Efficiency is most often quoted for planar detectors which are not in a position to detect the 1332 keV line of ^{60}Co .

Of these four measures of the efficiency of an HPGe detector, the second and the third are dependant on the geometrical relationship between the source and the detector. For the purposes of this report, peak efficiency is taken to be the *Absolute Full Energy Peak Efficiency* and the total efficiency is taken to be the *Absolute Total Efficiency*. With respect to the efficiency calibration of HPGe detectors, it is these two parameters that are of most interest and consequence in the quantitative analysis of samples or materials for gamma-ray emitting isotopes.

1.4. Determination of Detector Efficiency

For most laboratories, HPGe detectors are deployed for the routine determination of a limited number of radionuclides. In the situation where the laboratory could be sure that it would never need to measure activities of any other radionuclides quantification could theoretically (and perhaps optimally) be achieved by direct comparison of the response of the detector to a known amount of the isotope of interest with the response produced by the sample without ever having to establish the relationship between energy and efficiency that lies at the root of the normal efficiency calibration process. However very few laboratories are in a position to be certain as to the number of isotopes they will be required to measure and hence the requirement exists to establish efficiency values over a range of energies for which isotopes with appropriate gamma-ray emissions may not be available or practicable to use.

For quantitative measurements of gamma-ray emitting radionuclides, the full energy peak efficiency is the parameter of most significance and it may be calculated as:

$$\epsilon_{peak} = R / (S \times P_{\gamma}) \quad [3]$$

where R is the full energy peak count rate in counts per second, S is the source emission rate in Bq and P_{γ} is the emission probability for the gamma being emitted at that energy. The convention in gamma-ray spectrometry is to construct an interpolative curve by measuring gamma-rays at many energies covering the energy range of interest and plotting the full energy peak efficiency as a function of energy (a similar curve being often plotted for the total efficiency).

This is typically achieved by observing the response of the detector (the photopeak area) to known amounts of specific isotopes and calculating the efficiency. Selection of isotopes allows the efficiency to be interpolated over a range of energies. However for accurate results to be obtained, certain factors pertaining to the establishment of both peak and total efficiency values using such empirical methods must be taken into account. These factors relate to both the isotopes used, the geometry and the nature of the matrix within which the isotope of interest is contained.

1.4.1. Considerations for the Empirical Determination of HPGe Detector Efficiencies

Although the establishment of efficiency values for detectors may seem a relatively straightforward procedure, a number of considerations must be taken into account to ensure the applicability of the generated efficiency curve to the analysis of isotopes not used in the calibration process.

1.4.2 Sample Distance, Geometry, Density and Composition

The intensity of gamma-rays at a point some distance from a radioactive source is a function of distance as described by the normal inverse

square law. Use of this law requires information regarding the exact distance between the source and the point being considered. In practical gamma-ray spectrometry it is often relatively difficult to accurately establish the reference point with respect to distance as multiple scatterings within the active volume implies that the reference point is actually within the detector volume. The inverse square law can be used to deduce the distance experimentally. If R is the full energy count rate, then this count rate must vary according to:

$$R \propto 1/d^2 \quad [4]$$

where d is the sum of both the detector endcap to source distance, D , and the distance between the reference point within the detector volume and the detector endcap, d_0 . Thus equation [4] may be represented as:

$$1/R^{1/2} = kD + kd_0 \quad [5]$$

k being a constant. Equation [5] allows for the calculation of d_0 by measuring R at varying distances, D , and plotting one against the other, the intercept on the abscissa being the measure of d_0 . This value is not constant however and is a function of the energy of the incident gamma-ray photon, d_0 for low energy photons being less than for high energy photons which penetrate deeper into the active volume of the detector crystal. Such measurements will also indicate that for low values of D (close positioning of geometry relative to the detector), non-linearity will be observed. In summary, the inverse square law to determine efficiency for varying source to detector distances can only be applied where the distance d_0 has been calculated for each and every energy of interest and where the source to detector distance D is not small (due to true coincidence summation which is introduced later). The above discussion, although derived in

relation to a point source, can be applied to voluminous geometries although such extrapolation relies on assumptions being made about the distribution of activity within the source. In practice, calibration of a gamma-ray spectrometer is therefore usually confined to a fixed distance or a number of distances from the geometry to the endcap of the detector although empirical factors relating the efficiency at these distances may be calculated providing this is performed for all energies.

In reality, samples being measured by gamma-ray spectrometry are not usually presented to the detector in the form of point sources but rather as volumetric entities usually termed geometries. Although the calculation of the solid angle subtended by a detector to a point source is a relatively simple matter to calculate, such calculations are complicated for volumetric sources. This means that extrapolation of efficiency information for one geometrical form to another is too complicated to be practicable in daily use.

Related to this problem, but of a slightly less complicated nature is the problem of differences in fill height in cylindrical containers which tend to form the majority of commonly encountered analytical geometries. Such a case involves a correction to equation [5] such that:

$$1/R^{1/2} = kD + kd_0 + k_h \quad [6]$$

where b is the effective height of the sample within the geometry. If the geometry position is constant (axial and distance) equation [6] can be rewritten in the form $y = mx + c$ as:

$$1/R^{1/2} = K + kfH \quad [7]$$

where H is the actual source height within the geometry. Successive adjustment of the height of a liquid standard within the geometry can then be used to plot equation [7] and calculate the value of K and k_f . This then allows correction for fill height within a cylinder although large corrections may not be valid and such correction may not be correct for nuclides requiring corrections for true coincidence summation.

A subject of much discussion (and many proposed correction methods) is the phenomenon of self absorption of gamma-rays by the sample matrix itself. Typically, calibration of HPGe detectors is effected by presenting known amounts of activity to the detector in the chosen geometry. The activity is usually present in aqueous solution or distributed within one of the many water equivalent plastics available commercially. Both these matrices have a nominal density of 1.0. Problems arise when samples are presented to the detector with densities significantly different to the calibration matrix for which the applied efficiency curve has been established, especially for photons with energies less than approximately 100 keV. A correction may be made in a relatively simple manner using:

$$R_0 = R_{\mu} / (1 - e^{-\mu t}) \quad [8]$$

where R is the “raw” count rate in the peak of interest, t is the sample thickness and μ is the linear attenuation coefficient at the energy of interest and for the sample matrix being considered. Equation [8] however is complicated by the fact that μ is only valid for samples with one component. If the sample is a complex mixture (soils, etc.) then calculation of μ is complicated due to both the number of potential components in the mixture and the fact that the relative percentages of the components may not be known. Standard compositions for soils, vegetation etc. have been proposed by various organisations but the applicability of such

attenuation factors for the vast range of sample compositions that pass through a laboratory places some doubt on their universal applicability.

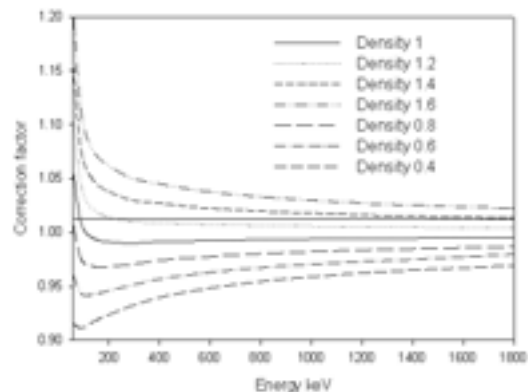


Figure 1.7. Plot of experimentally derived correction factors for soils of different densities to account for self-absorption effects. The correction factor is equal to

$$\epsilon_{\text{water}} / \epsilon_{\text{soil}}$$

A second consideration is that, especially for low energy photons, the chemical composition of the sample, irrespective of its overall density, exerts an influence on the self absorption of the photons by the sample. For samples of equivalent overall density, the samples with higher levels of metals such as Pb, Fe etc, will exhibit higher levels of self absorption than can be accounted for by density alone. Pertinent and in-depth discussion of the problems introduced in the previous section as well as various proposed methods for their correction are presented in Abbas et al. (2001), Galloway (1991), Bolivar et al. (1996), Fraczkiewicz and Walkowiak (1992), Tian et al. (2001) and Korun and Martincic (1992)

1.4.3 True Coincidence Summation

True coincidence summing is a problem whenever isotopes with complex cascades of gamma-rays are measured on a detector. Unlike random summation (in which two pulses arrive at the detector in a time less than the resolving period of the detector/electronics system), total summing is not count rate dependant but is

reliant on the source geometry and the relationship of the geometry to the detector. In particular, close to detector geometries, such as those typically encountered in environmental gamma-ray spectrometry where high efficiency is at a premium, are especially vulnerable to true coincidence summation.

True coincidence summation is a function of the probability that two gamma-rays emitted simultaneously by an isotopes decay will be detected simultaneously. The simultaneous arrival of two (or more) gamma-ray photons within the detector is heavily dependant on the solid angle subtended at the detector by the geometry holding the sample or source. Such simultaneous arrivals results in losses of counts from the true full energy photo peaks. Some of these counts lost from the photo peak may be found in sum peaks within the spectrum. Summing may also occur with partially absorbed photons resulting in backgrounds that are higher on the high energy side of the true photo peak than on the lower.

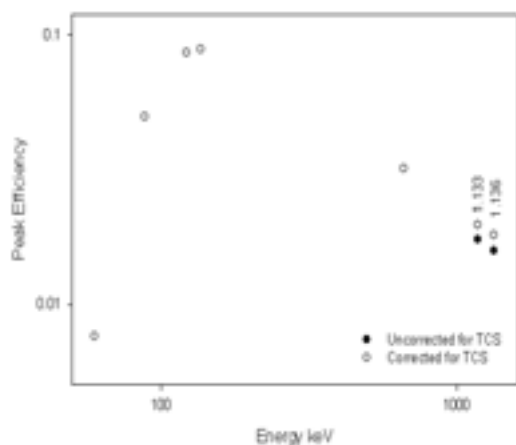


Figure 1.8. Experimentally derived efficiency plot incorporating ^{60}Co showing difference in efficiency values both with and without correction for true coincidence summation for a close to detector geometry. Factors applied to correct the efficiency are included over the relevant peaks.

It is true coincidence summation that limits the applicability of isotopes such as ^{152}Eu , ^{60}Co , ^{88}Y and ^{133}Ba to the establishment of efficiency

calibrations despite the large number of useful gamma-ray emissions from these isotopes. In close geometry situations such as those typically encountered in environmental laboratories, the efficiencies calculated using these isotopes in no way resemble the efficiency of a mono-energetic gamma emitter at the same energies. The phenomenon of true coincidence summation reduces the number of isotopes that may be used for efficiency calibration at close to detector distances. Isotopes that have no or negligible true coincidence summing are marked with an asterisk in Table I. Thus it can be seen that the two isotopes that provide high energy gamma-rays and are in common usage as calibration sources, namely ^{60}Co and ^{88}Y , are both vulnerable to varying degrees to true coincidence summing and therefore constitute a problem for the higher end of the usual energy range if this phenomenon is not taken into account in the calibration process. The most common way of avoiding such problems is avoidance of isotopes exhibiting true coincidence summation yet it is obvious that such an approach limits the range of energies which are available by using only isotopes not affected by the problem. The alternative is to correct for the problem during the calibration procedure. Suitable treatments of the problem and possible solutions are presented in Sinkko and Aaltonen (1985), Abbas et al. (2001) and Sima and Arnold (2000).

1.4.4 Curve Fitting

As previously presented, an accurate determination of the full photopeak efficiency is a prerequisite for the accurate determination of the analyte isotopes in samples presented to the detector. Conventional empirical determination of efficiencies is performed at a series of discrete energies corresponding to the gamma-ray emissions of the isotopes used in the calibration. To obtain the efficiency values for energies not used in the calibration, some sort of interpolation must be performed between the

calibration points (and extrapolation if the calibration is to be extended beyond the energy range over which the calibration sources emit gamma-ray photons). In order to respect the actual data points the interpolation must be made in some way that minimises the degradation of the actual data. This is usually achieved by fitting certain analytical functions to the data or alternatively but less commonly in recent times, plotting the curve by hand. As introduced earlier, conventional HPGe detectors display a characteristic efficiency curve which is most often plotted on a 3 cycle log – log graph. For energies up to approximately 130 keV the peak efficiency rises steadily if somewhat non-linearly (Fig. 1.9.) and after approximately 160 keV the peak efficiency falls away in an approximately linear fashion (on such a log-log plot). The maximum energy plotted using conventional empirical calibration methods is typically either 1332 keV from ^{60}Co or approximately 1800 keV from ^{88}Y . However it is typical that the calibration is often extrapolated out to 2000 keV or greater despite the fact that efficiency has been shown to tend to drop away faster than the usually applied linear relationship would suggest for energies greater than 2000 keV (Gilmore and Hemingway, 1996).

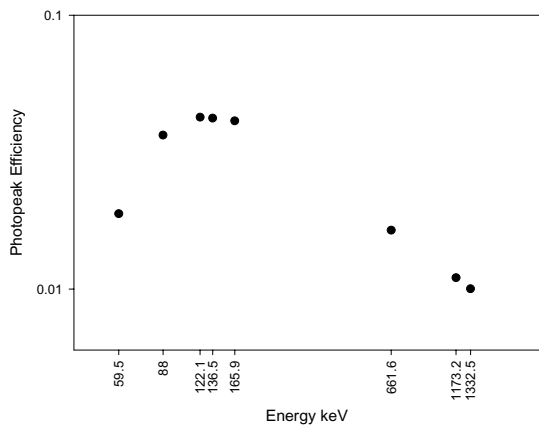


Figure 1.9. Typical photopeak efficiency curve for a *p*-type HPGe detector (log-log plot).

The functions used to describe the curves fitted to efficiency calibrations tend to belong to a relatively small group, some being depicted in Fig. 1.10.

Linear functions (known as such due to the absence of a log modifier on the energy data) are described by:

$$\log(\varepsilon_{peak}) = \sum_{i=-1}^n a_i (1/E)^i \quad [11]$$

where a_i is the coefficient to be determined and ε_{peak} is the photopeak efficiency at energy E . The order of the polynomial n is determined by the number of data points ($n=5$ for 10 or more, $n=4$ for 8 or 9, $n=2$ for 3 to 5).

Empirical functions are typically of the form:

$$\ln(\varepsilon_{peak}) = \sum_{i=0}^n c_i [\ln(c_a / E)]^i \quad [12]$$

where c_i is the coefficient to be determined, ε_{peak} is photopeak efficiency at energy E , c_a is a scaling factor calculated as $(E_2 + E_1)/2$ where E_2 is the highest calibration energy and E_1 is the lowest calibration energy.

After the efficiencies have been determined for the calibration peaks, a weighted least squares fit can be made to the polynomial expressions for both linear and empirical functions as described above. The difference of the shape of the efficiency curve for both low energies and high energies has predicated the use of dual efficiency curves in recent times. A “knee” or cross-over point is defined, typically between 130 and 150 keV, and two curves are drawn, one below the cross-over and one above. The functions are of the form:

$$\ln(\varepsilon_{peak}) = \sum_{i=0}^n b_i (\ln(E))^i \quad [13]$$

where b_i is the coefficient to be determined, ϵ_{peak} is the photopeak efficiency at energy E .

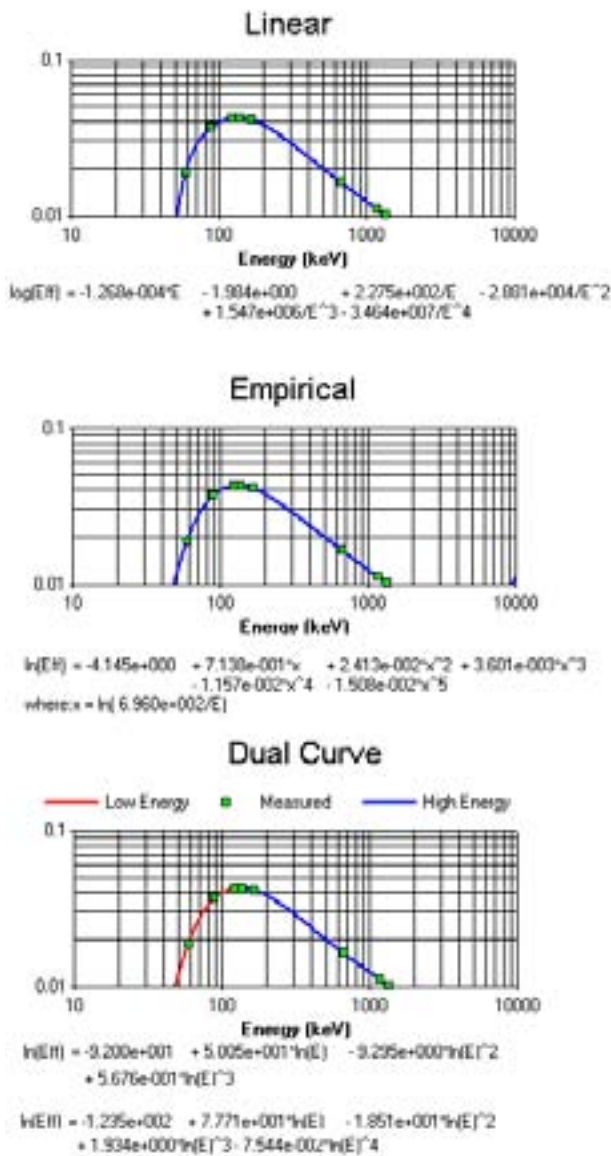


Figure 1.10. Depictions of three common functions for efficiency curve fitting as applied to the data of Figure 11.

1.4.5 Selection of Isotopes

Of some consequence in the efficiency calibration of HPGe detectors is the selection of isotopes used in the calibration process. The energy range of interest in the field of environmental monitoring or emergency response is typically between approximately 40 keV and 2500 keV. The calibration of an HPGe

spectrometer by calculating the detector response to known amounts of activity in defined geometries necessitates the use of a range of isotopes with gamma emissions in this energy range. Table I displays a number of the most commonly encountered isotopes with some information regarding energy, half-life and emission probabilities.

Other nuclides exist that may supplement this list although the practicability of many of these isotopes is limited by virtue of their short half-lives or limited availability. Some use has been made of isotopes such as ^{133}Ba and ^{152}Eu which exhibit a number of strong lines although strong coincidence summation for these isotopes has limited their general use. As can be seen from Table I, the energy range between approximately 50 keV and 2000 keV is quite evenly covered by commonly available isotopes although for energies greater than 2000 keV the situation is markedly different given the relative lack of practicable isotopes with emissions above this cut-off.

1.5 Current Procedures for Calibration of HPGe Detectors

At the time of writing, current procedures for the efficiency calibration of HPGe detectors at NRPA involve the determination of both full peak and total efficiency using a range of individual isotopes. The employed procedure involves a number of discrete steps some of which are typically found in such calibration procedures and some of a more advanced nature designed to overcome the problems highlighted in sections 1.4.1. through 1.4.5.

1.5.1 Preparation of standards

Certified solutions of individual isotopes are purchased and are used in the preparation of working standard solutions for the calibration procedure. The isotopes used in the procedure

are ^{241}Am , ^{57}Co , ^{139}Ce , ^{137}Cs and ^{109}Cd providing discrete energies between 59 keV and 1332 keV.

Isotope	T ^{1/2}	Energy keV	P _γ (%)
$^{210}\text{Pb}^*$	22.2 y	46.54	4.06
$^{241}\text{Am}^*$	432.7 y	59.54	35.9
$^{109}\text{Cd}^*$	462.7 d	88.03	3.65
$^{57}\text{Co}^*$	271.8 d	122.06	85.68
		136.47	10.67
$^{139}\text{Ce}^*$	137.6 d	165.85	79.9
$^{203}\text{Hg}^*$	46.59 d	279.19	46.59
$^{113}\text{Sn}^*$	115.1 d	391.70	64.89
^{85}Sr	64.84 d	514.01	98.0
^{134}Cs	754.3 d	604.69	97.63
$^{137}\text{Cs}^*$	30.25 y	661.66	85.20
^{134}Cs		795.84	85.52
$^{54}\text{Mn}^*$	312.3 d	834.84	99.97
^{88}Y	106.6 d	898.04	94.1
^{65}Zn	244.26d	1115.55	50.60
^{60}Co	5.27 y	1173.23	99.89
		1332.50	99.98
^{22}Na	2.60 y	1274.54	99.93
^{88}Y		1836.06	99.36
$^{228}\text{Th}^*$	698.2 d	2614.53	35.86

Table I. Most commonly encountered calibration isotopes.

At the time of writing, ^{88}Y is under consideration to extend the range to approximately 1800 keV. The solutions are diluted in appropriate carrier solutions to provide approximately 2 l of a working standard calibration solution of known massimetric activity.

The secondary standard solution is then dispensed gravimetrically into a number of plastic containers that constitute the analytical geometries currently used for analysis. These geometries range in volume from containers of some 26 mm in diameter holding some 20 mls to 550 ml Marinelli re-entrant beakers (Table II). The majority are cylindrical except for the

container designated U1 which is gently conical. For reasons discussed later, the Marinelli re-entrant beaker will not be discussed in the context of the mathematical calibration procedure presented later in this report.



Figure 1.11. Dispensing and dilution of standard isotope solutions for preparation of calibration geometries.

The activity in each geometry at the time of counting is determined and together with the net photopeak areas is used to determine the photopeak efficiency at the relevant energies (59.5, 88, 122.1, 136.5, 165.9, 661.6, 1173.2 and

1332.5 keV) and the total efficiency at appropriate energies.

Code	Max. Vol. (mls)	Dimesions (mm)	Volume (mls) and fill-height (mm)
W1	28	Height 29	14.0, 10
		Int. Dia. 42	28.0, 20
W2	105	Height 30	40.0, 10
		Int.Dia.73.5	80.0, 20
L1			
U1	500	Height 50	100.0, 13
		Dia 100-110	250.0, 30

Table II. Dimensions of analytical geometries and fill heights used in the calibration process.

Each container except the Marinelli re-entrant beaker is filled to two specific fill heights with each solution. The Marinelli beaker is filled to one specific fill height. The containers are then sealed and stored at temperatures designed to reduce evaporation prior to actual counting.

1.5.2 Counting of standards

Each container is then placed directly and coaxially on the endcap of the detector to be calibrated and counted for a period sufficient to ensure 100,000 counts in the photo peaks of interest after correction for background. The area of the photopeak is then determined using the software of choice. Total efficiency is determined as using all the counts present at energies less than that of the photopeak for single gamma isotopes.

1.5.3 Calculation of Efficiency

The determination of total efficiency for non-monoenergetic isotopes is complicated slightly

by the presence of two or more primary emissions but for the cases of ^{57}Co and ^{60}Co it is solved as follows.

For ^{57}Co total efficiency is calculated as below and expressed for 122.1 keV as this is the dominant emission.

$$\frac{C_{Total}}{(0.856A + 0.1068A)} \quad [13]$$

where C_{Total} is the total counts in the spectrum and A is the activity of ^{57}Co . For ^{60}Co the emissions are divided almost equally between the two energies. In this case the total efficiency is stated for 1252.8 keV (equidistant between the two emission energies) and it is calculated as follows:

$$\frac{C_{Total}}{(0.9997A + 0.9998A)} \quad [14]$$

The above calculations generate data for both the photopeak efficiency and the total efficiency for every isotope in every geometry at every fill height. Consideration of the earlier discussion indicates however that the photopeak efficiency values for ^{60}Co will be slightly depressed due to true coincidence summation, the amount of the depression varying with geometry. To correct for this fact, use is made of the program CSCOR (Sinkko and Aaltonen, 1985) to establish the correction factors for each geometry at the two energies of ^{60}Co . To perform the correction, curves are drawn, either by hand or using one of the common mathematical functions to the uncorrected peak and total data. The efficiencies at a number of specific energies are determined and then energy and efficiency data are entered into the CSCOR program to determine the appropriate correction factor. These factors are then applied to the corresponding peak efficiencies at 1173 and 1332 keV. The corrected

data is then used to establish the new peak efficiency curve.

Once the total efficiency curve and the corrected peak efficiency curve have been established, the relevant efficiencies for a range of energies out to 5000 keV are determined. A series of files are constructed for each geometry and fill height and used to determine the efficiencies at a fill height corresponding to 0 mm. This is achieved using a program called FIRHO to extrapolate the efficiencies at the two fill heights down to a fill height of 0. It should be noted that this process is performed for each fill height, i.e. an extrapolation to 0 is performed twice. Once this has been performed, the two data sets generated for a fill height of 0 are combined and an average of the two is calculated. This is performed for all geometries, both for peak and total efficiency. The end result of the process is a set of total and photopeak efficiency data for each geometry at a theoretical fill height of 0 mm. These files then form the basis for further analysis of samples.

1.6. Discussion

The previous section briefly introduced the concept of calibrating HPGe detectors for efficiency, the potential problems involved and current methods employed. It can be seen that traditional, empirical, laboratory based methods of efficiency calibration are restrictive with respect to sample geometry and type. The only samples that may be measured with any acceptable degree of accuracy are those that are presented in the same geometry as was used in the calibration or that vary from the calibration geometry in some respect that can be easily accounted for. It can also be seen that corrections must subsequently be applied for samples that deviate significantly from the calibration matrix with respect to density or matrix composition. The calibration process itself includes a number of potential pitfalls in relation to the problem of selecting available, practicable monoenergetic gamma-ray emitting

isotopes. A significant problem remains the fact that the two most commonly selected high energy gamma-ray emitting isotopes, ^{60}Co and ^{88}Y are both susceptible to the effects of true coincidence summation introducing the necessity for correction for the effects of this phenomenon in the calibration process. The calibration procedure currently employed serves to correct and ameliorate many of the problems described previously in an effective manner. The use of mainly monoenergetic sources eliminates the need to be overly concerned about the effects of true coincidence summation on the efficiencies calculated and in the case of ^{60}Co , steps are taken to correct for the effects of true coincidence summation for this isotope. The problem of having to match sample geometries exactly with calibration geometries in relation to fill height is also alleviated to some extent using methods similar to those previously described, the ultimate output of the process being efficiencies extrapolated to a fill height of 0 which allows for a certain flexibility regarding sample fill heights within the chosen geometries. The problem of matrix matching and density variation between samples and calibration sources is not dealt with during the calibration phase and is handled as part of the analysis procedure itself.

Currently, the energy range for the calibration extends out to 1332 keV although efficiencies are calculated out to a theoretical range of 5000 keV. Due to the extent of the extrapolation some consideration has been given to the use of ^{88}Y to extend the actual measured range out to approximately 1800 keV although this approach has concomitant problems relating to both the expression of total efficiency and correction for true coincidence summing. The validity and necessity of extending the calibration curve out to 5000 keV is a factor of some concern due to the fact that the most recent evidence suggests that the relationship between energy and efficiency at such energies cannot be simply

extrapolated out from data generated between approximately 600 keV and 1800 keV. Secondly, there is no simple way of checking the validity of efficiencies at this high energy range as the number of gamma emitting isotopes with emissions of higher than 3000 keV is very limited. Practically, the calibration procedure is a labour and time intensive operation involving the preparation and measuring of a large number of individual geometries for each individual detector. The preparation and measuring of these geometries constitutes a significant undertaking in terms of both man power and detector time and subsequent calculations also prove to be relatively time consuming.

In addition to this but of no less significance are considerations regarding the purchasing and use of radioactive solutions. Some of the isotopes used have relatively short half-lives and are not amenable to storage and are often only available from manufacturers at certain times of the year. This problem is exacerbated to some extent by the fact that the shortest lived isotopes used are those with emissions at the most crucial part of the calibration curve, namely between 80 and 150 keV and therefore cannot be realistically omitted. A significant amount of waste is generated in both the handling of the solutions and their ultimate disposal. In addition to this, preparation of the calibration solutions involves handling of chemically toxic solutions of a variety of metals and the handling of radioactive materials.

The above factors are of some pertinence with respect to the changing situation regarding emergency preparedness and measurements in emergency situations. In order to respond effectively to unforeseen emergency scenarios, a high degree of flexibility is necessary with respect to measurement capabilities. This flexibility is related to both the types of sample materials that can be analysed reliably, the ability to be able to compare results and utilize the

equipment, facilities and data of co-responders and to tailor analysis routines to the demands of situations as they present themselves. In addition, it is probable that such challenges during emergency situations will present themselves outside of the normal laboratory environment removed from the support facilities associated with that environment and under the time constraints imposed by the need for accurate data during such situations.



Figure 1.12. *The changing nature of the threats related to radioactive materials requires the ability to conduct activities in the field that would normally be carried out in a regular laboratory environment.*

Due to the above considerations, mathematical methods of calibration would appear to offer some advantages over laboratory based conventional procedures. Primarily these advantages are related to expense, flexibility and the ability to operate outside and independent of the normal laboratory environment. Factors such as these have precipitated a certain level of interest and work with respect to non- or semi-empirical calibration methods and such methods range from simple procedures to relatively complex and computationally intensive models of detector responses. The following section introduces the best known mathematical calibration procedures and describes a number of approaches that have been taken in the past.

2. Mathematical Calibration Methods

Although the theory behind the interaction of gamma-ray photons with matter, in this instance the detector and its surroundings, is quite well understood, the application of theoretical methods to the determination of detector efficiency is hampered by a number of factors. Predominant among these factors is the manufacturing process behind the production of HPGe detectors. This process is currently unable to produce standardized detectors with respect to the active volume of the crystal. As a result of this each detector is subtly different from all others and requires its own efficiency to be established usually by the means discussed in the earlier sections. Should it be possible to construct standardized detectors then the matter of establishing efficiency of any individual detector could be reduced to the tabulation of efficiency for a set of standard detector sizes and geometries in a similar manner to that conducted by Heath (1964) for scintillation detectors. Perhaps the first attempt at mathematical procedures for the calibration of HPGe detectors was the semi-empirical procedure proposed by Moens et al (1981) and elaborated upon by Moens and Hoste (1983). A three stage procedure, the method involved determining the efficiency of axially positioned reference point sources and then determining the solid angle of the desired source-detector configuration relative to the solid angle as defined for the reference source and the detector. Establishment of this ratio allowed correction of the reference peak efficiency to provide a value for the desired source – detector configuration. Although the method took into account various attenuation factors, the integrative process was extremely restrictive in relation to the range of geometries that could be calibrated for.

For low energy gamma-ray photons where the photoelectric effect is dominant (see Fig. 1.4.), the variation of efficiency with energy may be relatively well estimated using the product of the probability that the photon reaches the detector and the probability of its full absorption in the active volume of the crystal. Debertin and Helmer (1988) use this product to approximate the intrinsic efficiency of a Ge detector up to energies of approximately 70 keV using the relationship:

$$\varepsilon_{in} = 1 - e^{-\mu t} \quad [15]$$

where μ is the linear attenuation coefficient for Ge and t is the detector thickness. This model assumes either no interaction on passing through the detector or that all interactions contribute to the full energy photopeak. Interaction with endcaps and construction materials may be incorporated in the model using similar relationships to that of [15].

For higher energies where the two other primary processes (Fig. 1.4.) become relevant, the situation is complicated and no satisfactory relationship has yet been devised. The semi-empirical suggestions of Freeman and Jenkin (1966) and Harvey (1970) which incorporate all three processes, were unable to eliminate the need for empirical appraisal of the efficiency. This area has been revisited however with some success being reported for large volume HPGe detectors by Sudarshan and Singh (1991). A suite of methods that may offer some promise however are those most often described as Monte Carlo methods.

2.1. Monte Carlo Methods

The general Monte Carlo method is a computational technique for the solution of problems that depend on probability in some manner. Such procedures are typically used

where exact descriptions of a process may be impracticable to solve by direct methods for some reason. The Monte Carlo process uses a stochastic model that describes the process in question and a set of high quality random numbers is then used to sample the probability distribution functions as described by the model being used. For situations of the type being considered here (i.e. radiation transport) the probability distribution functions are defined by the interaction cross sections of interest.

Monte Carlo methods as applied to detector calibration are based on the simulation of individual photon histories and the tracking of photons from the source on their path through the detector and associated materials. As the photon passes through the detector material it undergoes a variety of interactions as described previously and produces electrons, positrons, and a full range of secondary photons such as bremsstrahlung, fluorescence radiation and annihilation particles. The Monte Carlo method then tracks each of these as they pass through the detector. At each and every point of interaction the probability of each interaction occurring is calculated and the potential scattering angles are incorporated to ascertain the final result of the interactions. As all events are followed through to their final condition, the entire spectral distribution is recreated.

The development and practical application of algorithms for the interaction of photons with detectors has seen a rapid growth in recent years. Many of these algorithms utilize Monte Carlo methods as such procedures are better suited for complex geometries and the multiple interactions that occur within the detector volume. The Monte Carlo method is fundamentally a computer based technique and its primary advantage rests with the degree of physical realism that can be attained in the mathematical description of the problem.

Monte Carlo modeling of photon interaction is a relatively common practice and has been reported upon in the literature since the 1970's (Atwater, 1972; Beattie and Byrne, 1972). These and subsequent studies have mainly produced two kinds of algorithms; complex codes which require relatively powerful computer resources and are relatively difficult to operate, and a suite of simpler algorithms created for more specific tasks which require less computing power but are of limited use and applicability. The enormous demand on computing power of the first type of codes is accompanied by a requirement for a high level of operator skill in preparing geometry and detector descriptions and ensuring that the codes are operated in a manner that will produce realistic results. The smaller codes tend to be so narrowly focused that their applications are severely limited, such codes often exhibiting overly simplified radiation transport models which may omit various important physical processes. Moreover, these codes are also often only valid for a certain type of source or detector or for a certain arrangement of these two relative to each other.

The deployment of Monte Carlo procedures for the calibration of gamma-ray detectors can be traced from its early application towards the problem of describing response functions for 3 x 3 inch NaI detectors. In the 1960's, Weirkamp (1963) discussed Monte Carlo procedures for the establishment of the photofractions and intrinsic efficiencies of a NaI detector for the coaxial placement of point sources at various distances. Beattie and Byrne (1972) used a Monte Carlo method for determining the response function of a NaI detector to monoenergetic gamma ray and the work of these researchers was expanded by Berger and Seltzer (1972) who calculated response functions taking into consideration such processes as multiple scattering and bremsstrahlung which had not been accounted for in previous work. The work involved gamma rays up to 20 MeV but was restricted to parallel

rays. The relationship between Monte Carlo determined efficiencies and empirically derived data for point sources and a cylindrical NaI detector out to 16 MeV and for a fixed distance was confirmed by Grosswendt and Waibel (1975).

As detectors based on semi-conductors began to achieve predominance in the early 1970's, the focus of attention had shifted towards the application of Monte Carlo methods to the calculation of efficiencies for such detector types. Wainio and Knoll (1966), De Castro Faria and Levesque (1967) and Peterman et al. (1972) reported on the application of Monte Carlo methods to the determination of efficiencies for semi-conductor detectors and as methods were developed, the methods were applied to non-point sources and detectors of various size and shape. Kushelevski and Alfassi (1975), Vano (1975), Somorjai (1975), Haase et al. (1993) and Winn (1993) report on various extensions and modifications of Monte Carlo methods towards problems relating to volumetric sources and different geometrical shapes such as Marinelli beakers.

The above authors, on comparison of calculated results with empirically derived efficiency values, obtained agreement generally within 10% and sometimes 5%. An empirically derived efficiency value typically has an uncertainty of the order of 3% and the higher uncertainty associated with the Monte Carlo methods reduced their applicability in the earlier period of their implementation. The higher uncertainty associated with the Monte Carlo values arises from a number of factors. With reference to early attempts to employ such methods, perhaps the most significant factor was the statistical limitation associated with the method. A Monte Carlo code that simulates physical processes related to the dissipation of a photons energy within the detector in the absence of an unreasonable number of simplifications or

assumptions requires a not insignificant amount of computer processing time if the statistical uncertainty associated with each event is not to be too large. The problem is of course exacerbated for larger crystal sizes and for photons of higher energies. As an example, for a photon of 3 MeV with a medium sized detector, 10^5 individual photons must be tracked to produce an uncertainty of the order of 2%. The large number of calculations involved and the limited processing power of computers in the 1970's and 1980's limited the application of Monte Carlo methods due to the unrealistic amount of time required to produce uncertainties that are required in the calibration of Ge detectors. This factor however has reduced in significance with the increase in recent years of computing power and low uncertainties can now be achieved in a practicable period of time using readily available computers.

The second factor relates to the detector itself. Despite modern manufacturing methods there remains significant uncertainty with respect to the active volumes of individual Ge detectors. Although manufacturers can provide information regarding the physical size of individual detectors, uncertainties remain regarding insensitive regions of the detectors, in particular with respect to the dead layers at the contacts. These uncertainties can be reduced to some extent by the use of radiography to allow direct measurement of crystal dimensions and using a large number of simulations, that would have been unfeasible 30 years ago, to achieve the best agreement between the calculated and empirically derived efficiency values.

The third factor relates to the nuclear data used in the calculations Mass attenuation coefficients used in determining the interaction of photons with matter typically had uncertainties of the order of 5% up to the 1980's and the uncertainties could be considerably worse for

factors related to photoelectric and Compton interactions. The quality of such data has improved in recent years as a result of concerted effort regarding the quality and evaluation of nuclear data.

It should also be realized that comparisons of empirically derived and computational efficiency values are vulnerable to how the full energy photopeak area is determined. Modelled peak areas may include counts that occur in the low energy tail of an experimentally derived photopeak and which subsequently may not be included in the empirical peak area measurement. This difference in relation to which counts are used in the measure of efficiency can lead to some discrepancy when comparing empirical and calculated values.

2.1.1. Monte Carlo Codes

Currently, the two predominant codes used in Monte Carlo determinations of Ge (and other) detector efficiencies are MCNP (Monte Carlo N Particle) and GEANT4. Both of these packages are general purpose transport codes that may be used in a variety of different scientific fields and are therefore relatively complex. It is therefore common to find that a large number of packages have been developed to simplify the use of these codes for various purposes (health physics, reactor design, dosimetry etc.) but the underlying code for these packages is most often either MCNP or GEANT4 (or one of the previous iterations of either code).

MCNP, originally developed and currently maintained by the Diagnostics Applications Group of Los Alamos National Laboratory in the United States, is a general purpose, continuous energy, generalized geometry, neutron/photon/electron transport code that can be used in a variety of modes including neutron only, photon only or electron only or various combinations of these three, the photon energy range being from 1 keV to 100 GeV.

MCNP uses nuclear and atomic data drawn from the Evaluated Nuclear Data File system (ENDF) and the Evaluated Nuclear Data Library (ENDL) system. Data is processed for use in MCNP in such a way as to retain the integrity of the original data files. MCNP includes photon interaction tables for all elements from $Z=1$ to $Z=100$. For the purpose of establishing detector response functions, the user creates an input file that is subsequently read by MCNP. This file contains information about the problem such as:

- * the geometry specification
- * description of materials, detector etc.
- * specification of the photon source,
- * the type of answers desired,
- * any variance reduction techniques to improve calculation efficiency

The complexity of these files and their potential for impacting on the quality of the desired output has been perhaps the driving force behind the development of user-friendly interfaces to the MCNP code.

The other code most often found as the basis for software designed for the implementation of Monte Carlo procedures in relation to gamma ray spectrometry is GEANT4. GEANT4 is an object-orientated toolkit designed for the simulation of the passage of particles through matter. The development of GEANT 4 can be traced to studies completed by the European Laboratory for Particle Physics (CERN), in Geneva and the High Energy Research Accelerator Organization (KEK) in Tsukuba, Japan with respect to the implementation of advanced computing techniques to the already existing GEANT3 codes (development of the original GEANT codes began in 1974). The resulting workgroup, RD44, was a collaboration of scientists from 10 nations and the first release of GEANT4 was in 1998 with the GEANT4 working group being formed in 1999 with a view

towards the further development and maintenance of the code.

Also used to some extent is the Electron – Gamma Shower (EGS) code, a general purpose package for the Monte Carlo simulation of the coupled transport of electrons and photons in arbitrary geometries for particles with energies between 10 keV and TeV's. Developed by a group at the Stanford Linear Accelerator Centre at Stanford University in the U.S., the EGS code proper was first introduced in 1978 as version EGS3 and the first iterations of the code did not include photons with energies below 100 keV. The current version of the code, EGS4, includes the features:

- radiation transport of electrons or photons in any element, compound or mixture,
- inclusion of Bremsstrahlung,
- multiple scattering,
- pair production,
- Compton scattering,
- Photoelectric effect.

Since the release of EGS4 a variety of additions have been made including graphical interfaces and the extension of the code to lower energies. Further information on the EGS code system may be found in Ford and Nelson (1978) and Rogers (1984)

2.2. VGSL (Virtual Gamma Spectroscopy Laboratory)

The Virtual Gamma Spectroscopy Laboratory (VGSL) is a software package developed within the structures of the Comprehensive Test Ban Treaty and is designed to simulate data acquisition using the sort of HPGe detectors typically used in environmental analyses. The software allows for input of detector, geometry and shielding parameters and produces, among other things, both computed peak and total efficiencies out to 2500 keV . The software uses

a modified version of the MCNP code and as of version 3 of VGSL, MCNP version 2.5e was the

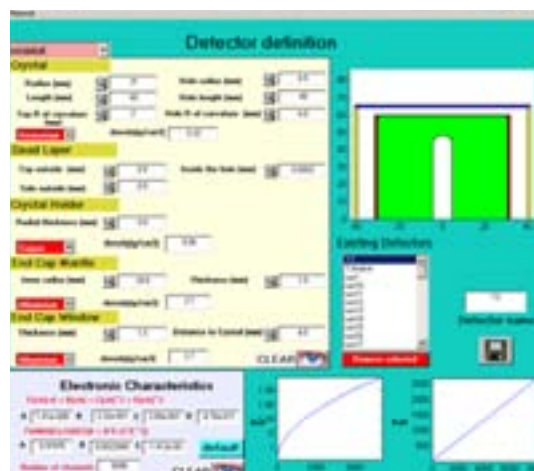


Figure 2.1. Detector parameter input screen of VGSL.

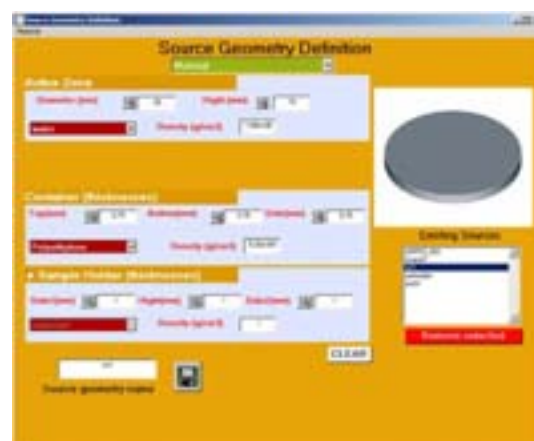


Figure 2.2. Geometry parameter input screen of VGSL.

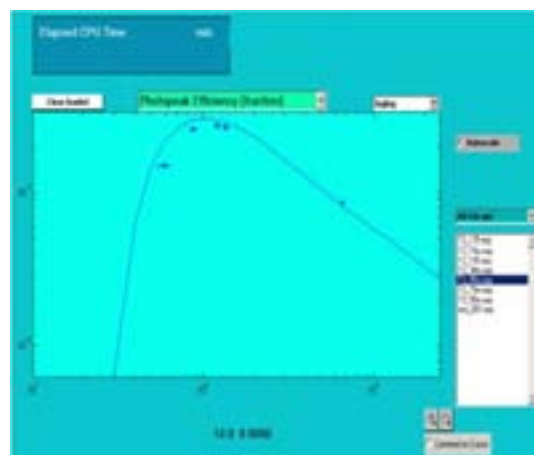


Figure 2.3. Output screen of VGSL.

code used. The version used in this study was v. 1.2. A full description of VGSL is to be found in Plenteda (2002). VGSL provides a convenient graphical interface to the MCNP code and removes the necessity for the time consuming construction of the files normally used by MCNP for the description of geometries and detectors.

3. Experimental

Unless otherwise stated, all sources used in this study were traceable reference standards from either the Physikalisch-Technischen Bundesanstalt (PTB) in Germany or the National Physical Laboratory of the United Kingdom. All simulations were performed on the detector as described in 3.1. and all work was conducted at the NRPA laboratories at Tromsø, Norway. All nuclear data used in the study was drawn from either Chu et al. (1999) or, for the determination of internal conversion coefficients, the tables of evaluated data maintained by the Laboratoire National Henri Becquerel in France. Spectra were obtained in all cases using Genie 2000 from Canberra Industries, analysis of spectra being conducted by in-house gamma spectrometry analysis software.

3.1. The Detector

The detector used throughout this study was a standard p-type HPGe detector (Model GC4019) from Canberra Industries and is denoted as T3 throughout this report. The nominal specifications of this detector were FWHM of 1.82 keV at 1332 keV, relative efficiency of 40.7% and a peak to Compton ratio of 66.8:1. The detector was cooled using an electronic cryogenic unit as opposed to more conventional liquid nitrogen. Shielding of the detector consists of 55 mm thick low background lead with a graded tin-copper lining

for the reduction of fluorescent lead x-rays. The detector is used for the routine determination of gamma-emitting isotopes in environmental samples.

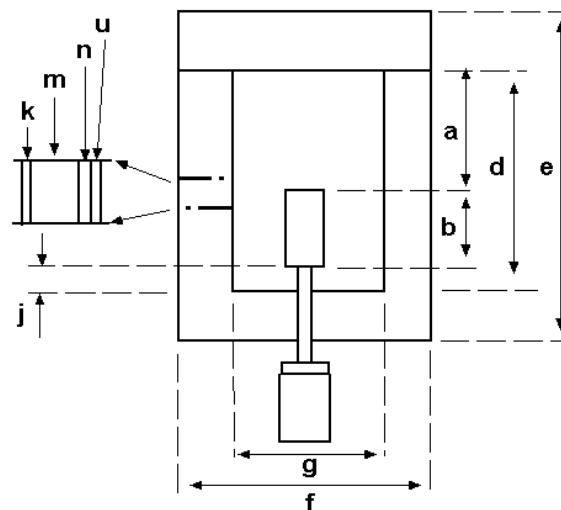


Figure 3.1. Shielding configuration for HPGe detector T3. a- 225 mm, b-147 mm, d-345 mm, e-505 mm, f- 360 mm, g-250 mm, j- 23 mm, k-1 mm aluminium, m- 55 mm lead, n-1 mm tin and u-0.7 mm copper. Dimensions not to scale.

3.2. Characterisation of the Detector

As discussed previously, the determination of efficiencies for HPGe detectors using Monte Carlo methods is reliant to a large extent on the correct characterization of the detector with respect to a number of aspects, most particularly in relation to the physical dimensions of the detector crystal and its active volume that usually cannot be provided with sufficient accuracy by the manufacturers, the dimensions and properties of the surrounding materials and certain aspects related to the configuration of the crystal within the detector housing itself. Nominal values for the detector dimensions were obtained from the manufacturer, the dimensions obtained being displayed in Figure 3.4. The detector was also subjected to a tomographic scan at Bærum Hospital in Norway in order to confirm some of the dimensions

supplied by the manufacturer, and to check for significant misalignments of the crystal within the housing. Although nominal values for all necessary dimensions were provided by the manufacturer, the fact that some of these dimensions are of special significance to the Monte Carlo process necessitated further characterization of the detector.



Figure 3.2. Computerised tomography of detector T3

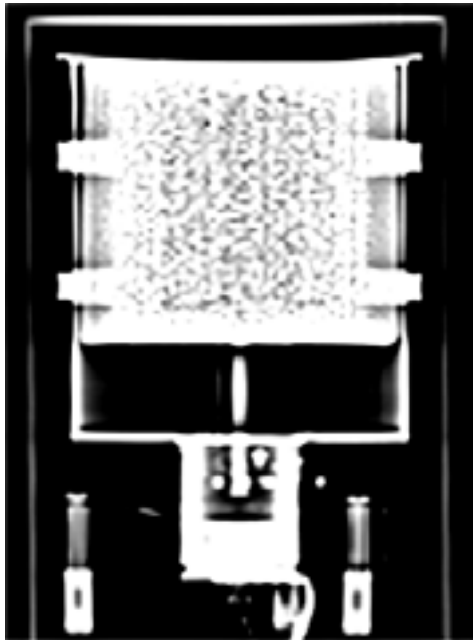


Figure 3.3. CT scan of detector T3

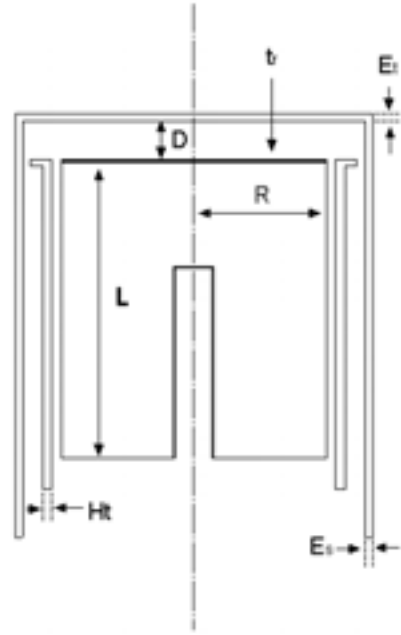


Figure 3.4. Nominal dimensions for detector T3. Ge crystal to end cap inner surface distance ($D=4.5\text{mm}$), Ge crystal radius ($R=31\text{mm}$), Ge crystal length ($L=60\text{mm}$), Ge front dead layer ($t_f=0.5\text{mm}$), hole radius ($r=4.5\text{mm}$), inner dead layer ($t_b=0.3\mu\text{m}$), hole length ($l=48\text{mm}$), holder thickness ($H_t=0.8\text{mm}$; Cu), endcap top thickness ($E_t=1.5\text{mm}$; Al), endcap side thickness ($E_s=1.5\text{mm}$).

3.3. Shielding

The shielding model of VGSL consists of a cylindrical 3 or 4 layer graded shield model with selectable shielding materials. The shielding of the detector used in this study consists of a graded shield (lead, tin, copper) square in plan. To convert this to a cylindrical shield with radius r , equivalent to the average distance between detector centre and the sides of a square shield of side length $2a$, the following was used:

$$r = \frac{4}{\pi} \cdot \ln(\sqrt{2} + 1) \cdot a \quad [16]$$

3.4. Point Source Measurements

The empirical phase of the optimization process involved the making of a series of measurements using certified points sources at a number of

fixed distances from the endcap, the sources being positioned coaxially and normal to the plane as described by the endcap surface. The point sources used were obtained from PTB and were as follows with activities quoted for the date on which measurements were made: ^{241}Am (94.1 kBq), ^{133}Ba (51.9 kBq), ^{109}Cd (100.82 kBq), ^{152}Eu (49.9 kBq), ^{57}Co (34.9 kBq), ^{137}Cs (73.1 kBq), ^{60}Co (19.03 kBq) and ^{22}Na (47.4 kBq). All sources had stated uncertainties of less than 1.5% and were mounted in the usual PTB configuration except for ^{109}Cd which was mounted in a Mylar mount to reduce absorption of its low energy x-rays. The sources were mounted over the detector using the device depicted in Fig. 3.5.



Figure 3.5. Measurement of point sources for detector characterisation.

This arrangement allowed precise positioning of the source over the detector with respect to distance and radial position. Distances were measured using a vernier micrometer from a convenient point on the endcap surface. Each source was measured for a period of time sufficient to ensure not less than 100000 counts in the smallest photopeak of interest. Each count was made 3 times and the average of all three counts used. Measurements were made at

the following distances: 35 mm, 55 mm, 75 mm, 95 mm, 135 mm and 195 mm. It should be noted that all measurements were made on the detector in the absence of the normally present shielding. Simulations were then run for each point source at each of the distances employed to ensure that the agreement between calculated and empirical efficiency was maintained over the distances.

3.5. Simulation of Volumetric Sources

In order to ascertain the how the Monte Carlo simulations performed in relation to the simulation of efficiencies for volumetric sources, empirical measurements of efficiency were obtained for a series of traceable volumetric sources (PTB) and these were compared to the results of Monte Carlo simulations performed using the parameters derived for the point sources. The first series of sources analysed consisted of polyethylene cylindrical boxes of the form denoted W1.

	KH854	KH861	KH860	KH856
Radius (mm)	21	21	21	21
Height (mm)	20	10	20	20
Density (g/cm ³)	1.0	2.0	1.6	0.5
^{54}Mn	3.58	3.60	3.55	3.60
^{60}Co	59.43	60.23	59.28	60.23
^{65}Zn	3.43	3.43	3.38	3.43
^{137}Cs	73.98	75.07	73.87	75.07
^{241}Am	87.32	88.61	87.12	88.61
^{109}Cd		64.66	63.60	64.66

Table III. Volumetric sources used to test Monte Carlo simulations of detector efficiency. Activities are given as Bq/source on the day of measurement. Activity uncertainties are less than 3% in all cases.

These were filled to either 10 mm or 20 mm (14 mls or 28 mls) with materials of varying density homogeneously spiked with a series of gamma emitting isotopes. Each source was counted for 48 hours and the peak efficiency determined in the normal manner. Each geometry was then modeled in VGSL and the peak efficiency of the detector for that geometry simulated. The sources used are described in Table III.

3.6. Calculation of Efficiency Transfer Factors without Detector Characterisation

Although the direct determination of detector efficiencies is the primary goal in the implementation of Monte Carlo procedures to gamma-ray spectrometry, it is possible to use Monte Carlo simulations to extrapolate empirically derived efficiencies from one geometry to a range of others without the characterization of the detector with respect to optimum dimensions. The testing of this approach was conducted by establishing a “reference” geometry which constitutes a baseline and whose efficiency information may be extrapolated out to other geometries.

The peak efficiency for a geometry of interest can be obtained from such a procedure using:

$$\varepsilon_i = \varepsilon_r / (S_r / S_i) \quad [17]$$

Where S_i and S_r are the modeled peak efficiencies for the geometry being investigated and the reference geometry respectively ε_r is the empirically determined peak efficiency for the reference geometry and ε_i is the transferred peak efficiency for the geometry being investigated.

In this instance, the reference geometry was point source at 35 mm distance from the

endcap. Using the nominal detector specifications without optimization, Monte Carlo simulations were run for this geometry and for the other desired geometries. The relationship between the efficiency values for the reference geometry and for the desired geometries was then used to modify the empirically derived efficiency values for the reference geometry and produce efficiency values for all the desired geometries.

3.7. A priori Determination of Total Coincidence Summation and Matrix Correction Factors'

As noted earlier, the impact of total coincidence summation constitutes a limitation on the accuracy of measurements of isotopes vulnerable to the phenomenon unless corrected for. Monte Carlo simulations of the interaction of photons from specific isotopes and the detector along with nuclear data for such isotopes allow for the determination of summation factors in advance of any measurement. With respect to matrix correction factors, as has been noted previously, any deviation with respect to density or matrix between the calibration standard solution/matrix and that of the sample introduces errors in activity determination. Although a variety of procedures and methods are documented in the literature many involve precision point measurements or are intended for laboratory implementation. Monte Carlo simulations that directly model the composition of the sample may offer significant advantages in respect to the calculation of such factors.

Total coincidence correction factor determination was assessed using ^{60}Co and ^{22}Na , two isotopes strongly affected by the phenomenon. Using point sources the deviations of the empirically derived peak efficiencies of a number of the isotopes' lines from the efficiency curve established using non-affected isotopes and Monte Carlo simulation were used to

establish empirical correction factors. The spectra from the same sources were simulated both with and without coincidence summation in order to determine modeled correction factors and these were analysed relative to empirical values. A series of volumetric sources were also used. The correction factors for these sources for ^{60}Co were determined using the CSCOR program as described in Sinnkko and Aaltonen, (1985). The correction factors determined thus were compared with those derived by Monte Carlo spectrum simulation.

	Soil 1	Soil 2	Soil 3	Cellulose	Steel
H	2.2	10.0	0.36	6.22	
O	57.5	78.0	49.62	49.33	0.45
Al	8.5		7.1		
Si	26.2		27.38		
Fe	5.6		4.38		98.93
C		11.4	2.14	44.45	
S					
Na			0.84		
Mg			1.6		
S		0.6			
K			2.37		
Ca			4.21		
Mn					0.62
Density	1.6	1.45	1.6	0.45	7.86

Table IV. Percentage elemental compositions and densities of selected matrices for the determination of density correction coefficients.

Matrix and density correction factors were determined by simulating various sources and matrices by the Monte Carlo procedure and then comparing the correction factors with those determined for a volumetric source by an alternative mathematical method utilizing linear attenuation factors for the matrices and materials used. A source consisting of water in the container described in this report as W2 was

chosen as the reference geometry with a fill height of 10 mm. The ranges of energies chosen covered the entire range typically encountered in monitoring or emergency measurements. The program GAMATOOL (AEA Technology) was used to determine correction factors for the efficiency of the detector for various materials relative to an aqueous calibration standard. The method used was that of Debertin and Jianping (1989).

Factors were determined for 3 different soil types, 2 being “wet” soils, the third being a dried soil sample. The other matrices were cellulose and steel. Details of the matrices and their composition are included in Table IV. Once the factors had been determined by the above method, simulations were run for each of the matrices presented in the chosen geometry. The simulated efficiencies were then expressed relative to the efficiencies determined for the aqueous matrix to determine the Monte Carlo correction factor.

4.0 Results and Discussion

4.1. Modeling of Detector Efficiencies

The analysis of the tomographical scan of the detector indicated that some of the nominal manufacturer's parameters with respect to the detectors dimensions may not have been in full agreement with the real situation. Based on the scan, the following dimensions were used to describe the detector for the preliminary Monte Carlo simulations: Ge crystal to end cap inner surface distance ($D = 8$ mm), Ge crystal radius ($R = 30.6$ mm), Ge crystal length ($L = 58.5$ mm), Ge front dead layer ($t_f = 0.5$ mm), hole radius ($r = 4.5$ mm), inner dead layer ($t_b = 0.3$ μ m), hole length ($l = 48$ mm), holder thickness ($H_r = 0.8$ mm; Cu), endcap top thickness ($E_t = 2.0$ mm; Al), endcap side thickness ($E_s = 1.5$ mm). It should be noted that due to the nature of the scan, the distance D could only be determined to within ± 2 mm and the midpoint of the two possible distances was used as the starting point for simulation. Some parameters could not be checked on the scan and for the initial simulations these were held at the nominal values. The parameters in question included those pertaining to the inner hole of the crystal and the front dead layer of the crystal.

After the detector parameters had been entered, a number of simulations were run to further optimize the simulation. In all cases, the measurements taken at 35 mm were used as a benchmark as it was for this configuration that uncertainties in both distance to the detector and axial position were judged to be lowest. The end cap to crystal distance, D , was modified to best describe the efficiency at 661 keV which is to a large extent not affected by the magnitude of the dead layer at the front of the crystal. Once the simulation provided a good approximation of the efficiency at 661 keV, the dead layer parameter, t_f , was modified to best approximate

the efficiencies at 59 keV and 88 keV. The analysis indicated that the efficiency of the detector was best simulated by extending the parameter D out to 9 mm and the parameter t_f to 0.85 mm from a nominal measurement of 0.5 mm.

Running the simulations using the nominal values indicated a large scale discrepancy between measured and calculated efficiency values (Fig. 4.1). This discrepancy in efficiency was largest for low energy photons being up to 70% of the empirical value at 59 keV, the discrepancy being maintained (albeit at lower levels approaching 10%) out to 1000 keV. Using the dimensions obtained from the scan of the detector improved the situation somewhat although good agreement between computed and measured values could only be obtained by extending both the dead layer at the front of the crystal and the distance between crystal and endcap as discussed above. It should be noted that it is unlikely that the dead layer at the front of the crystal is either uniform in thickness across the front of the crystal or that the transition between dead layer and active detector is immediate or uniform. The measure of the dead layer used in the simulations is therefore best viewed as an average over, at least, the front of the crystal.

The optimized detector description was used to simulate the detector response to the point sources at various distances and good agreement was obtained between simulated values and empirical data for all distances (Fig. 4.2). At the furthest distance of 19.5 cm it was considered that true coincidence summation effects would be negligible and the simulated efficiency curve was compared with data obtained from a large number of different energies (including those arising from ^{60}Co , ^{152}Eu , ^{133}Ba and ^{22}Na). The simulation provides good agreement for all energies over the range, none of the energies displaying the effects of true coincidence summation.

For 122 keV and 136 keV there appears to be a slight but consistent overestimation of peak efficiency values for all distances between source and endcap although this overestimation does not exceed 3% of the empirical value. A consistent slight underestimation of peak efficiency is also evident for the 661 keV photopeak at all distances. Once a satisfactory model of the detector had been obtained using the empirical efficiency data at 35 mm source-detector distance, simulations were run for all the distances at which point source measurements had been made. The results of the simulation of peak efficiencies at these distances are displayed in Figure 4.2. Data is only presented for singlet peaks unaffected by true coincidence summation. As can be seen from the data, good agreement was obtained between simulated and empirical data at all distances. In the majority of cases, under- or over-estimation of the peak efficiency values are consistent for

all distances as is apparent for the 661 keV peak and the 59 keV peak. It is possible that this reflects systematic errors introduced in how the empirical efficiencies are determined.

The Monte Carlo process does not take into account modules of the detector-electronics system that could theoretically affect the determination of the peak efficiency value. Peak tailing may, for example result in a lower empirical efficiency determinations as some counts are omitted in the determination of the peak area. It is also worth considering that counts may be lost from the peak due to random summation with the high count rates involved or aberrations in the peak may result in deviant determinations of the continuum under the peaks.

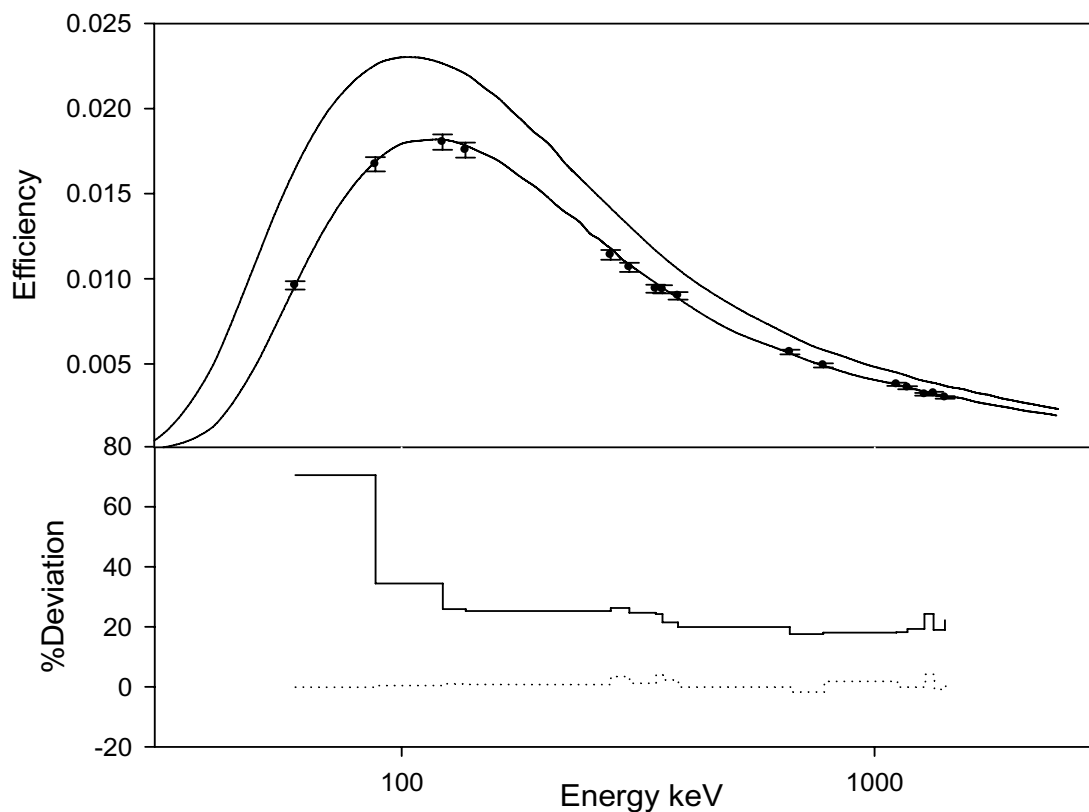


Figure 4.1. Plot of two Monte Carlo derived peak efficiency curves compared to empirically derived efficiencies (points) for the nominal detector dimensions (top curve) and optimised dimensions (bottom curve). The bottom graph represents the deviation (computed – empirical as a percentage of the empirical) for both nominal and optimised detectors as a function of incident photon energy.

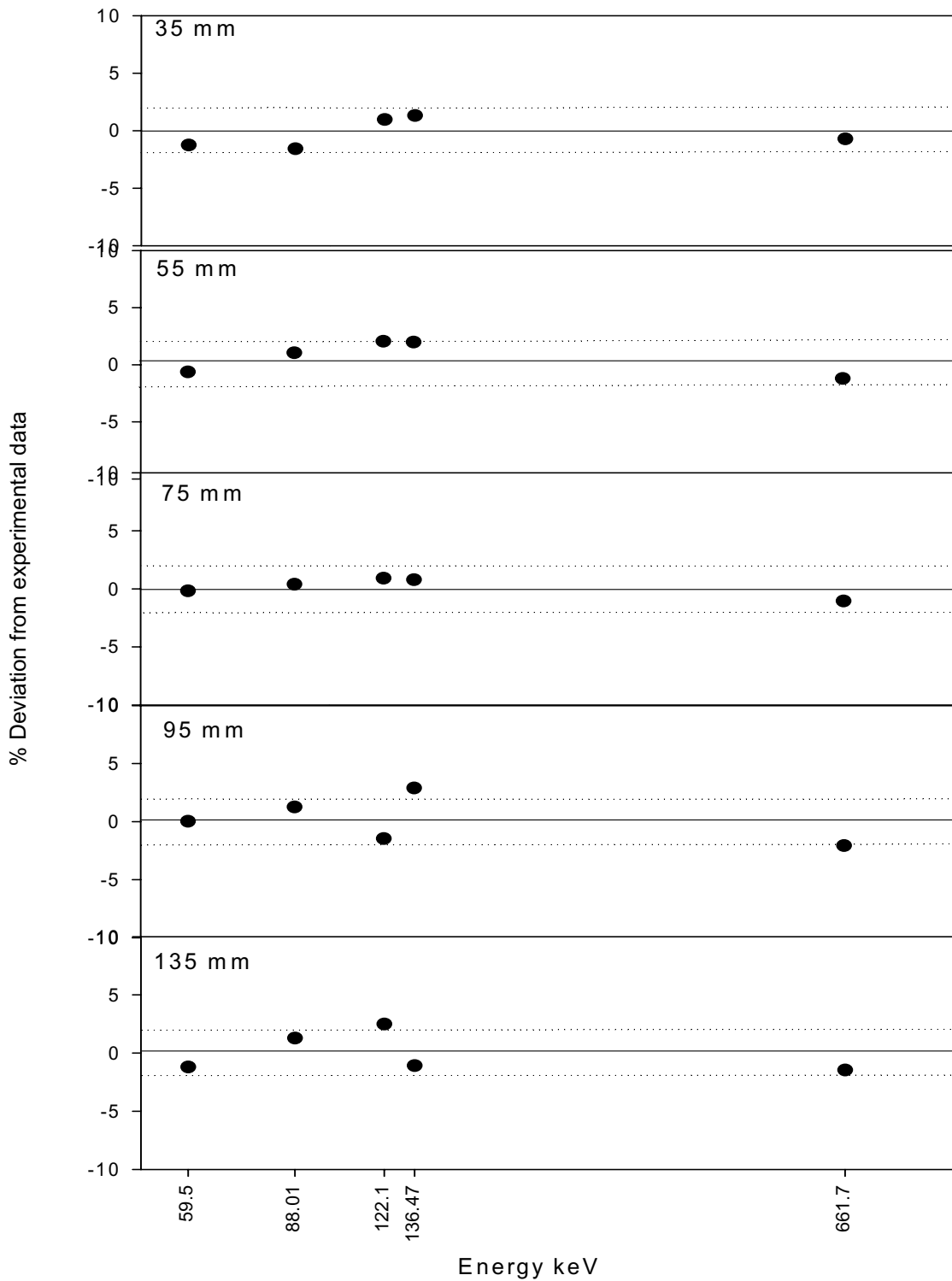


Figure 4.2 . Deviations of calculated peak efficiency values from empirical data (calculated – empirical as percentage of empirical) for point sources at increasing distance from the detector endcap for various photon energies. Dashed lines are 1σ uncertainties in empirical values.

Despite such considerations, it is clear from the results that it is possible to model the peak efficiency characteristics of the detector to within less than 4% of empirically derived data, a value that is comparable with uncertainties in peak efficiency values derived using conventional methods with subsequent efficiency curve interpolation. Such an uncertainty level is sufficient to allow for normal environmental measurements and more than acceptable for determinations conducted in the field or for emergency purposes. The empirical measurements made at 195 mm constitute a special case in that at such distances the effects

of true coincidence summation can be considered negligible for the majority of the isotopes used in this study. Figure 4.3. displays modeled peak efficiency values as a function of energy compared with empirically derived data. Agreement at all energies is very good being within the combined uncertainty associated with the empirical data. Although the simulation of peak efficiency values for the elementary case of coaxially positioned point sources provided acceptable results, to be truly practicable the method must be able to calculate efficiency values for the situation most often encountered in monitoring and emergency situations, that of

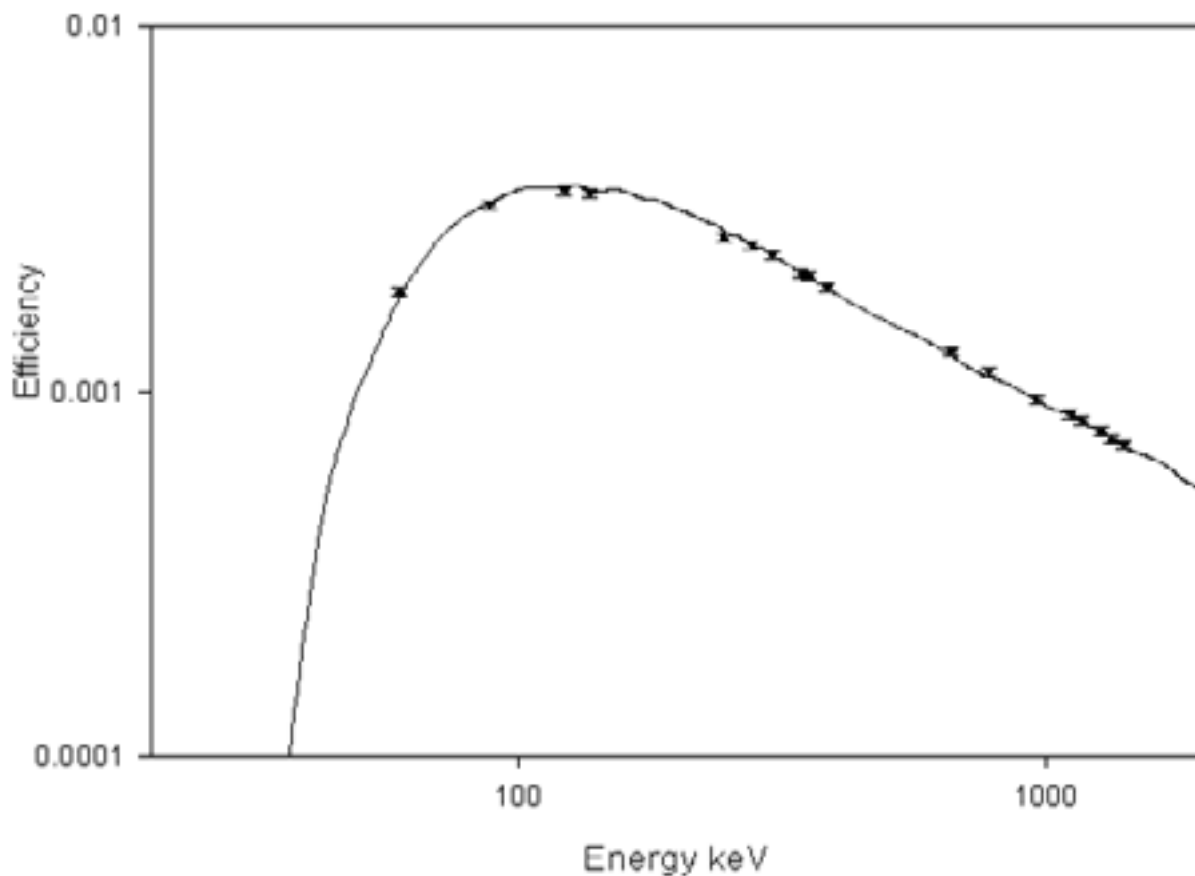


Figure 4.3 . Calculated peak efficiency curve for point sources at a distance of 195 mm from the detector endcap and empirical data including emissions from ^{133}Ba , ^{60}Co , ^{22}Na and ^{152}Eu normally vulnerable to true coincidence summation.

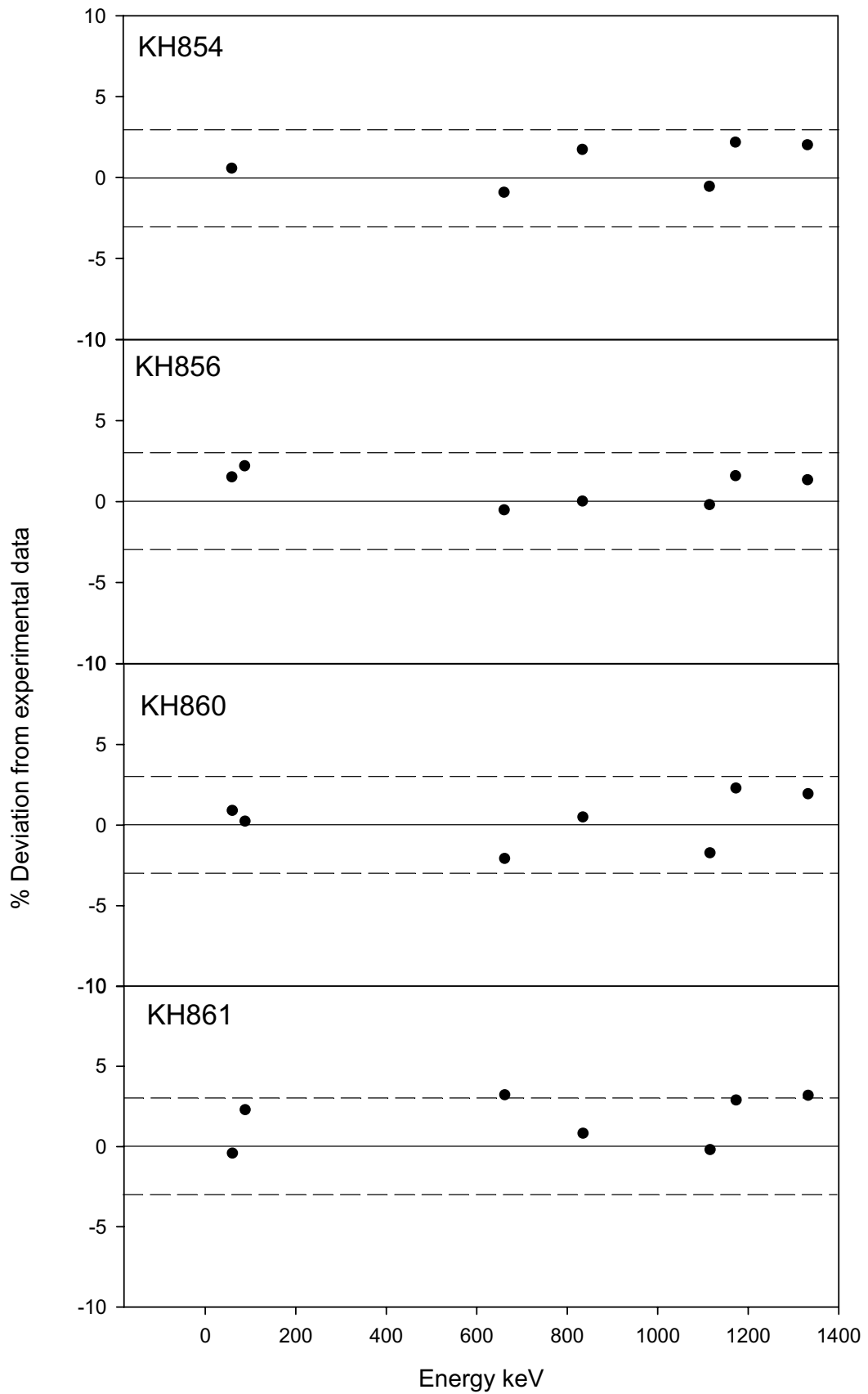


Figure 4.4. Deviations of calculated peak efficiency values from empirical data (calculated – empirical as percentage of empirical) for volumetric sources of various compositions as described in Section .. Dashed lines are 1σ uncertainties in empirical values.

measurement of volumetric sources of diverse density and composition. An appraisal of the efficacy of the procedure for such cases was conducted using the four volumetric sources as outlined in Section 3.5 and the optimized detector model. Figure 4.4 displays a comparison between empirically derived peak efficiency values for 4 different volumetric sources and the values determined by the Monte Carlo procedure. In all cases the deviation between modeled and empirical values are less than 4% of the empirically derived value. No significant deviations were observed related to density or composition of the sources and it is therefore concluded that the detector model and the Monte Carlo procedure are able to adequately model the detectors response with respect to peak efficiency for sources of various configurations and compositions.

Although it has been demonstrated that it is possible to model peak efficiency values, to be truly practicable as an alternative to laboratory based conventional calibration methods, the procedures must be able to adequately reproduce the total efficiency of the detector (i.e. the response of the detector to photopeak photons and those in the Compton spread). The situation with respect to appraisal of the procedures abilities with respect to total efficiency is complicated to some degree by two factors. The first of these is that there is only a limited range of energies available to determine and test calculations of total efficiency, these being those associated with isotopes emitting either mono-energetic gamma radiation or two gamma ray energies with simple decay schemes. The second factor is that while peak efficiency is essentially determined by the detector and its construction, external factors may affect the total efficiency of the detector by scattering of radiation back into the active volume of the detector.

A preliminary consideration of the problem indicated that there was a possibility that the

Monte Carlo simulations would not reproduce the total efficiency of the detector with a level of accuracy comparable to that attained for peak efficiency primarily for the second reason outlined above. The approach of Helmer et al (2004) was therefore adopted in order to correct for possible discrepancies introduced by the Monte Carlo procedures inability to fully include all the factors that could affect the total efficiency of the system. The total efficiency of the detector was modeled for each of the point source – detector configurations as used for the peak efficiency determinations. Comparison of empirically derived and modeled total efficiency values indicated an unacceptable discrepancy and it was therefore deemed necessary to correct the total efficiency values.

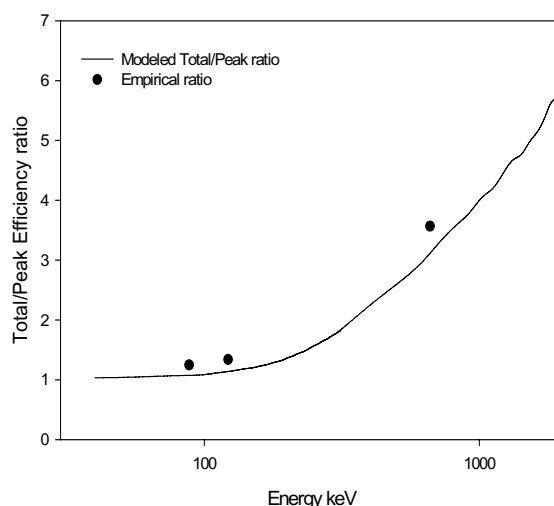


Figure 4.5. Deviation between empirically derived Total/Peak efficiency ratios and modelled ratios as a function of energy for point sources at 135 mm source – detector distance.

In order to achieve this correction, the total/peak ratios as empirically derived were plotted against the modeled ratios to observe the offset between modeled and empirical (Figure 4.5). An energy independent correction was then applied to shift the modeled curve to more

approximate the empirical data (Fig. 4.6). The factor was then used to correct the modeled total efficiency value by adding the corrective constant to the total/peak ratio and then multiplying by the peak efficiency to obtain the corrected total efficiency.

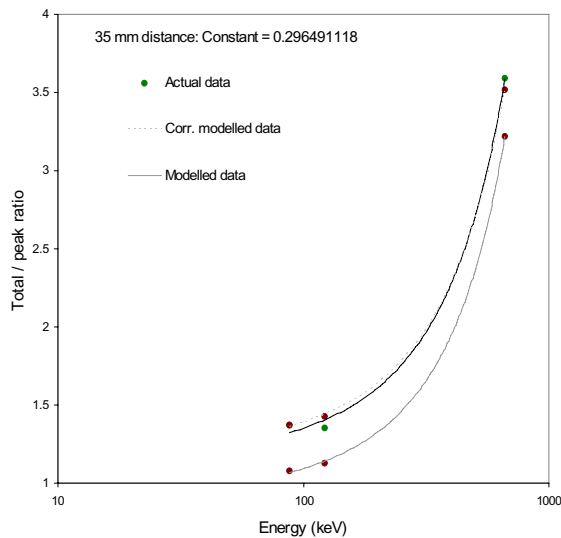


Figure 4.6 Correction of modelled total/peak ratios to closer approximate empirical data.

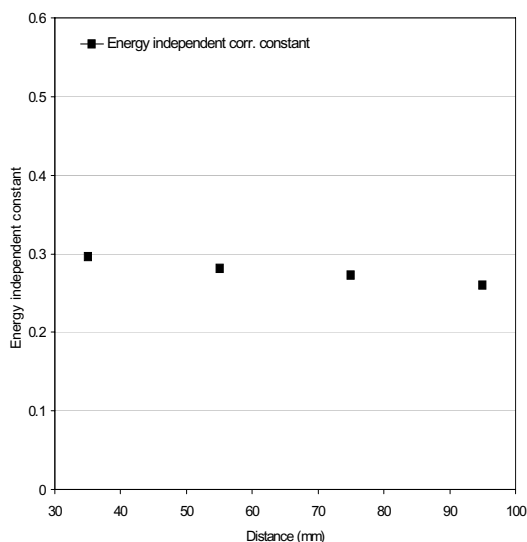


Figure 4.7 Variation of applied correction factor with distance of source from endcap.

Such an approach is of course dependant upon the Total/Peak efficiency ratio being independent of, in this case, distance. In order to test this, the correction factor was calculated for the total/peak ratios at various distances in order to observe the deviation (Fig. 4.7). Some variation can be observed with respect to distance although it would appear that over short distances the correction factor varies by relatively small amounts when considered in relation to the uncertainties introduced within the empirically derived data points.

4.2. Efficiency Transfer

The extrapolation of detector efficiency values from single well-defined reference geometry to other geometries using Monte Carlo procedures without prior detector characterization offers a relatively uncomplicated way of utilizing the advantages of the process without the slightly more complicated process of detector characterization. In this study, the reference geometry chosen was a point source at 35 mm coaxial distance from the detector endcap. The empirically derived peak efficiency for a number of point sources at different distances were then compared to the reference geometry (Fig. 4.8). Simulations were then conducted using the nominal detector characteristics without optimization and the modeled ratios of the peak efficiencies of the test geometries to those of the reference geometry were analysed relative to the empirically derived ratios.

A similar process was conducted for volumetric sources of varying compositions, the reference geometry being the source KH854 as described in Section previously. For volumetric sources the sources were positioned coaxially and directly upon the endcap as opposed to the varying distances of the point sources. It should also be noted that in this instance, not only is a geometrical variation involved but also compositional.

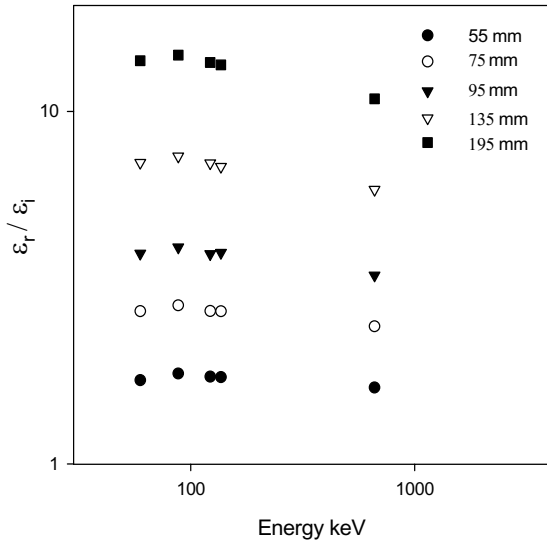


Figure 4.8 Relationship between empirically derived peak efficiency values for the reference geometry at 35 mm (ϵ_r) and those for point sources at various distances (ϵ_p).

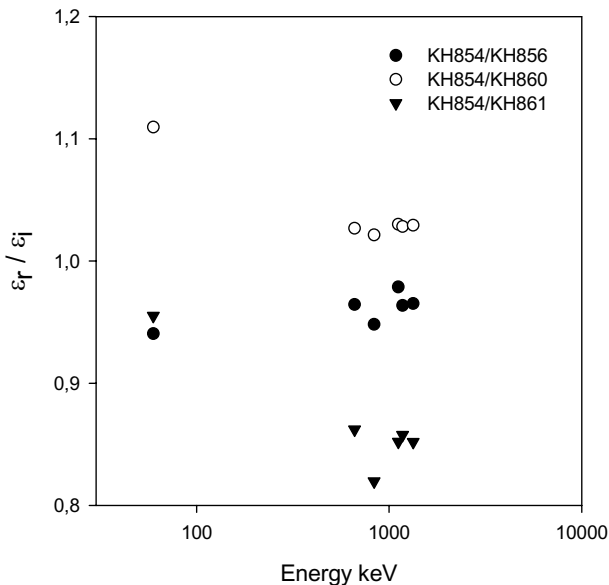


Figure 4.9. Relationship between empirically derived peak efficiency values for the reference geometry KH 854 (ϵ_r) and those for other volumetric sources (ϵ_p).

Results for both processes are displayed in Tables V and VI. In both instances, the transferring of efficiency from a reference geometry, be it either point or source, using only

the nominal detector dimensions resulted in better efficiency values than simply modeling of the efficiency using nominal detector dimensions but in no case were the results comparable with those produced by direct modeling using optimized detector dimensions. Nonetheless, for point sources with the worst case scenario (transferring efficiency from a near detector position to one farther away) the results only deviated from the actual empirical efficiency by approximately 10%. Such a factor may be acceptable in certain situations involving emergency measurements. Regarding volumetric sources, the situation with sources KH856 and KH860 was acceptable, the deviations between the empirical data and the values produced by the efficiency transfer were of the same order as those produced by direct modeling with optimized detector dimensions. It should be borne in mind however that these sources differ from the reference geometry only with respect to density and composition.

The method did not produce acceptable results for the KH861 source which differs from the reference with respect to both density and the height of the active volume. Based on this observation it would appear that implementation of such a transfer procedure would require more work for its application to anything more than the elementary case of point sources at various distances or possibly with respect to the derivation of efficiency values for samples that vary only in composition or density from the reference source. The results are in broad agreement with the recent EUROMET 428 project (Lepy et al., 2001) which investigated the use of various routines including Monte Carlo for the determination of efficiency transfer factors. The study indicated that best results are obtained for direct modeling of efficiencies using optimized detector models, the order of magnitude of the deviations obtained using nominal models and efficiency transfer routines being comparable to those observed in this study for point source measurements.

Energy keV	Deviation between empirical value and modelled value (nominal detector dimensions)					Deviation between empirical value and efficiency transfer value (nominal detector dimensions)				
	55 mm	75 mm	95 mm	135 mm	195 mm	55 mm	75 mm	95 mm	135 mm	195 mm
59.54	-74.24	-70.54	-66.71	-61.94	-60.30	3.94	5.98	8.09	10.72	11.63
88.04	-39.71	-34.46	-32.69	-29.78	-28.71	0.97	4.69	5.94	8.01	8.76
122.06	-31.13	-25.32	-24.02	-22.48	-21.02	2.65	6.96	7.93	9.07	10.16
136.47	-30.68	-25.26	-26.10	-20.12	-19.62	2.41	6.46	5.83	10.30	10.67
661.65	-22.32	-17.55	-15.08	-15.69	-8.54	2.70	6.49	8.46	7.98	13.66

Table V. Comparison of disparities between empirical data and data produced by direct Monte Carlo calculations using nominal detector dimensions and data produced by an efficiency transfer using nominal detector dimensions for point sources. In all cases disparity is calculated as empirical-calculated as a percentage of the empirical value.

Energy keV	Deviation between empirical value and modelled value (nominal detector dimensions)			Deviation between empirical value and efficiency transfer value (nominal detector dimensions)		
	KH856	KH860	KH861	KH856	KH860	KH861
834.85	-36.80	-36.70	-8.35	2.36	2.42	22.66
1173.24	-38.59	-37.87	-14.54	1.03	1.55	18.21
1332.50	-38.78	-38.79	-14.37	0.17	0.16	17.73
1115.54	-37.37	-34.68	-10.56	-0.77	1.20	18.90
661.65	-36.35	-33.00	-10.23	0.21	2.66	19.33
59.54	-98.95	-94.18	-42.58	-1.68	0.76	27.13

Table VI. Comparison of disparities between empirical data and data produced by direct Monte Carlo calculations using nominal detector dimensions and data produced by an efficiency transfer using nominal detector dimensions for volumetric sources. In all cases disparity is calculated as empirical-calculated as a percentage of the empirical value.

4.3. Density-Matrix Correction Factors

The correction of efficiency data due to disparities between calibration standards and actual samples remains a significant and commonly encountered problem with respect to conventional laboratory based calibration procedures. The problem is exacerbated to some extent by the likelihood of encountering various sample materials in emerging emergency

corrections although a significant number of them are reliant upon point source transmission measurements or they do not exhibit enough flexibility to be used outside the range of materials normally encountered in environmental monitoring laboratories. Monte Carlo procedures offer a possible solution via the modeling of efficiency data for various samples and materials. Table VII presents correction factors calculated using two methods for a number of sample types ranging from an

Direct Calculation						Monte Carlo Calculation				
Energy	Soil 1	Soil 2	Soil 3	Cellulose	Steel	Soil 1	Soil 2	Soil 3	Cellulose	Steel
40	1.38	1.06	1.43	0.92	24.25	1.42	1.08	1.43	0.94	22.99
60	1.14	1.05	1.15	0.94	8.34	1.13	1.05	1.15	0.93	8.62
100	1.06	1.04	1.06	0.95	2.90	1.06	1.05	1.06	0.94	2.97
200	1.04	1.03	1.04	0.96	1.60	1.04	1.03	1.03	0.96	1.64
670	1.02	1.02	1.02	0.98	1.28	1.04	1.03	1.02	0.98	1.33
1170	1.02	1.02	1.02	0.98	1.21	1.03	1.01	1.01	0.99	1.22
1670	1.01	1.01	1.01	0.98	1.17	1.03	1.02	1.01	0.99	1.22
2470	1.01	1.01	1.01	0.99	1.15	1.02	1.01	1.01	0.99	1.13

Table VII. Comparison of density-matrix correction factors for a variety of sample materials calculated using both direct determination using linear attenuation coefficients and Monte Carlo simulations.

organic material of low density to solid steel. Both methods produce values in good agreement with each other the disparities being naturally less as the energy tends towards higher values. The largest disparity between the methods is exhibited for the extreme case of steel although it should be pointed out that the method using linear attenuation coefficients can produce erroneous results if the dimensions of the sample are much greater than the free pathlength of the relevant photon in the material being corrected for. In this case, low energy photons less than 100 keV have free pathlengths in steel of less than 0.5 mm and the sample model used in the calculation had a thickness of greater than 10 mm which may account for the deviation between the results for the two methods.

4.4. Spectral Simulation

An aspect of the Monte Carlo approach of some use with respect to gamma-ray spectrometry is the ability to simulate various types of spectra of isotopes and sources as would be exhibited by the detector, once the efficiency characteristics of the relevant detector have been described. As the spectra are mathematical simulations of the detector, it is possible to modify them by various

means to display different aspects of the spectra or to manipulate various conditions. Figure 4.10 displays a simulated ^{133}Ba spectrum over the energy range up to 400 keV. As can be seen in the lower spectrum it is possible to simulate the spectrum with optimum resolution allowing investigation of features typically not seen in spectra taken with regular HPGe detectors. In this case the two contributions of the doublet peak, normally observed as a singlet, at 80 keV can be clearly seen with the higher resolution. The accuracy of the spectral simulation was assessed by recording an actual spectrum of a ^{60}Co source at 95 mm distance, a distance deemed far away enough from the detector to avoid any spectral distortion due to the high count rates that would have been recorded at nearer distances. A time normalized component from the laboratory background spectrum was added to the modeled spectrum to simulate the background present in the actual spectrum. As can be seen from Figure 4.11 the simulated spectrum is in excellent agreement with the actual spectrum in relation to the major features, all pertinent spectral components being accurately reproduced. The fine detail of the simulation is displayed in Figure 4.12 where it can be seen that the simulation produces a slightly narrower peak than in actuality and does

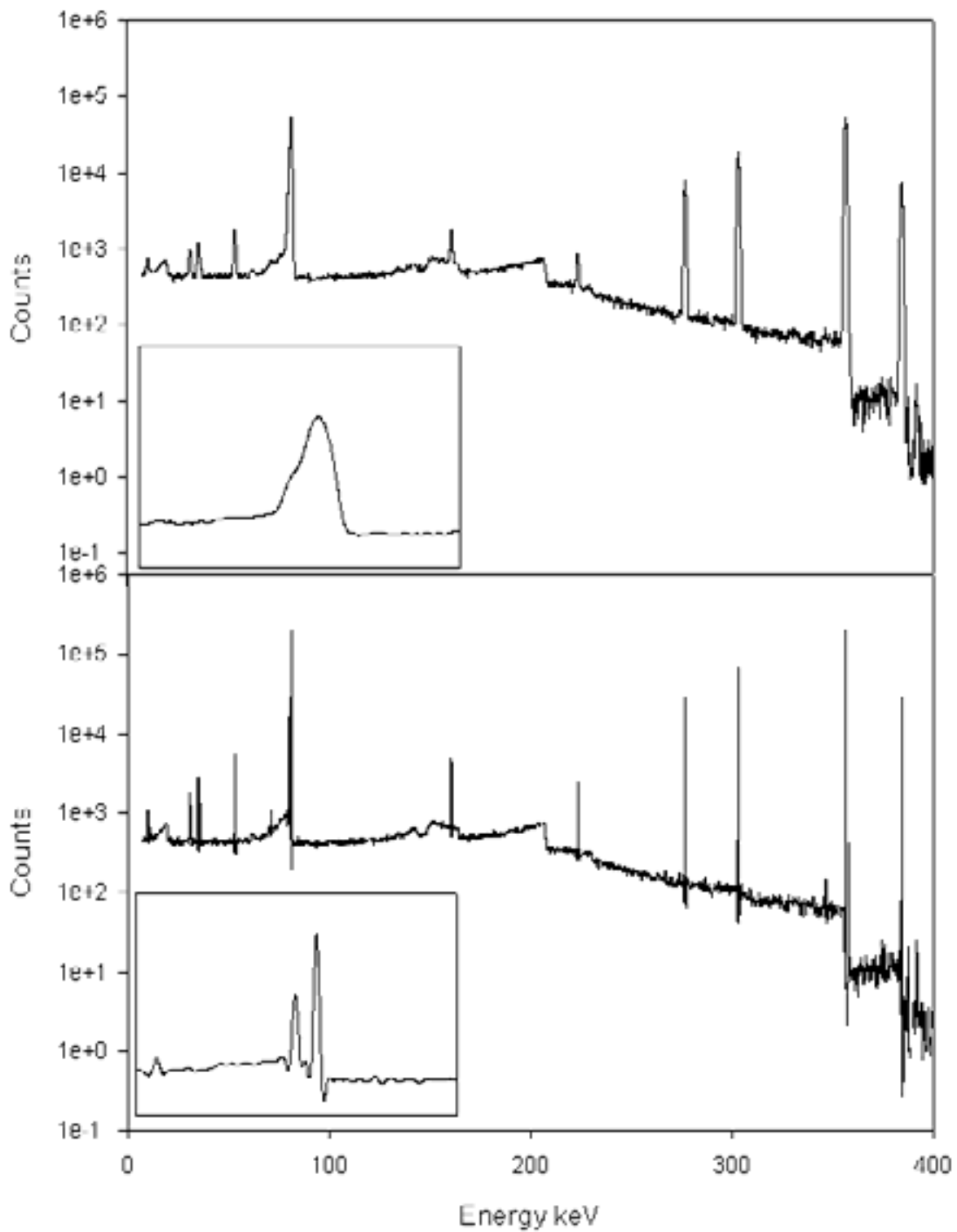


Figure 4.10 . Simulated ^{133}Ba spectra for detector T3 between 0 and 400 keV. Top spectrum simulated with normal resolution, bottom spectrum displaying the same information but simulated with a FWHM of 1 keV. Insets in both spectra display the doublet peak at 79.6 and 80.9 keV.

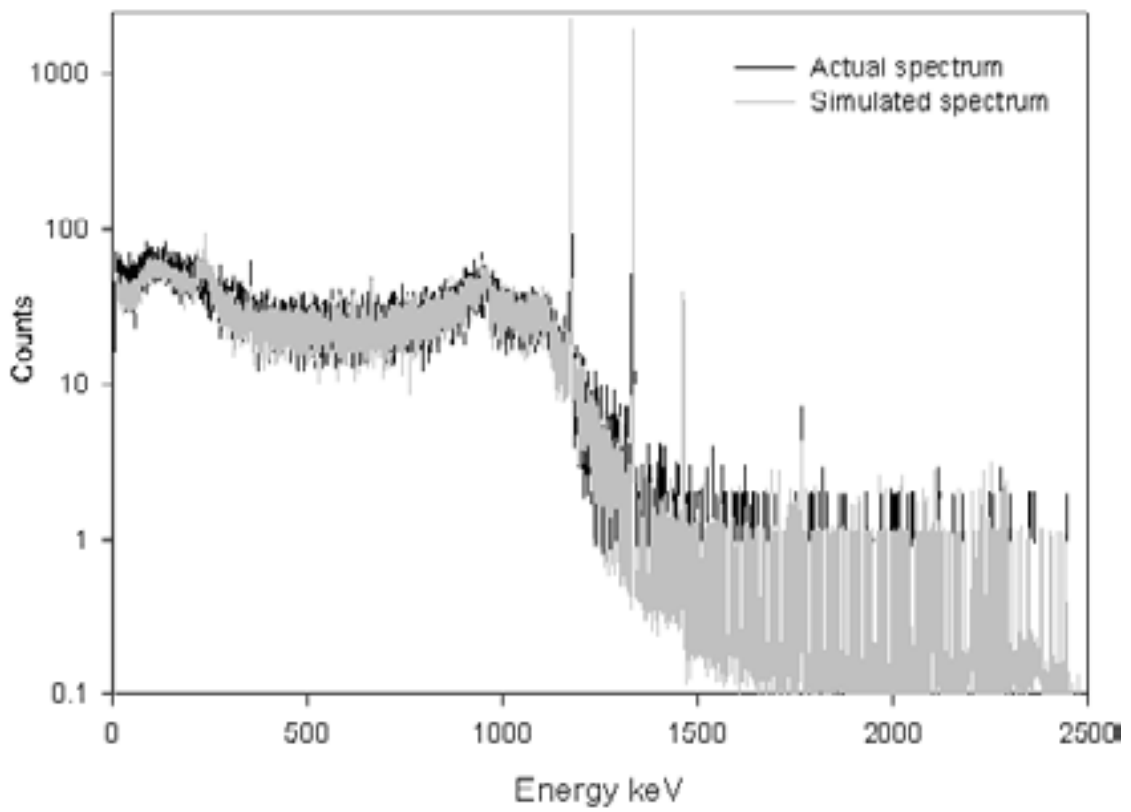


Figure 4.11. Simulated and real spectrum of a point ^{60}Co source at 95 mm.

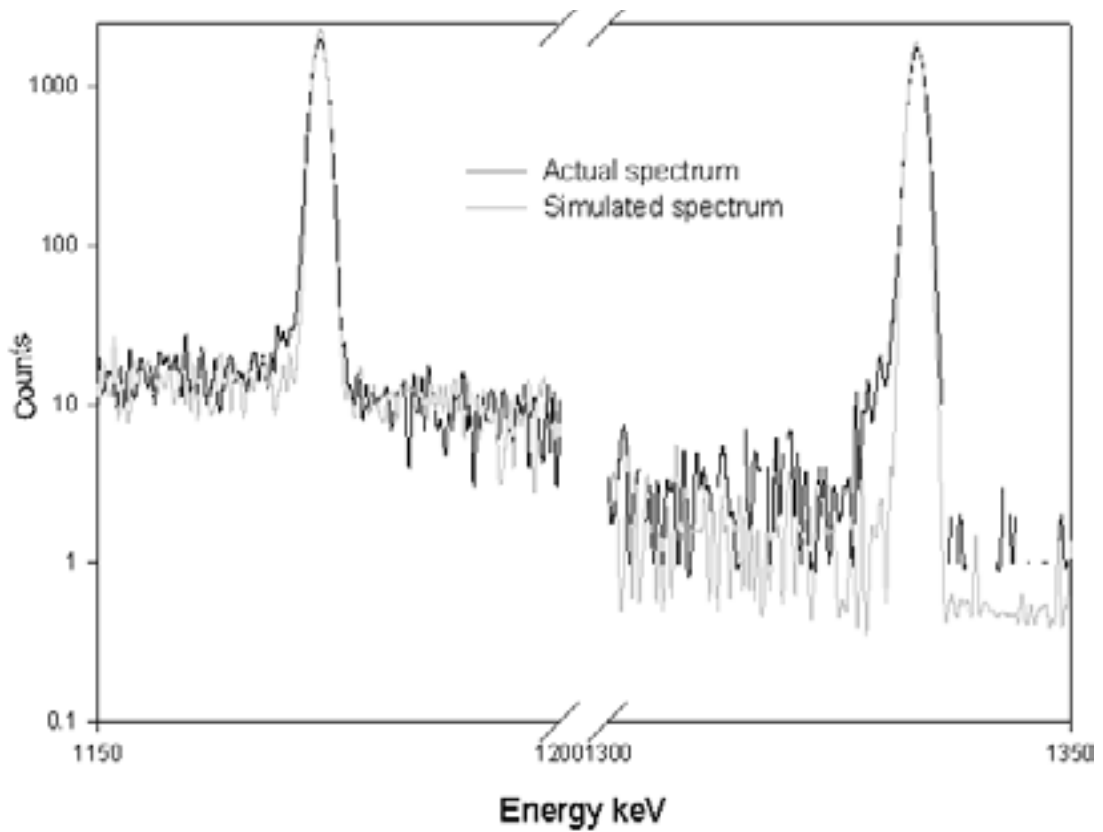


Figure 4.12 Close up of real and simulated ^{60}Co photopeaks

	Empirical		Modelled	
	1173 kv	1332 keV	1173 keV	1332 keV
Area	11803	10886	11601	10542
FWHM	1.822	1.900	1.584	1.772
FWTM	3.444	3.533	2.997	3.223
Gaussian Ratio	1.036	0.998	1.037	0.997

Table VIII . Comparison between important spectral parameters with respect to the modeled and empirical spectra for the ^{60}Co point source.

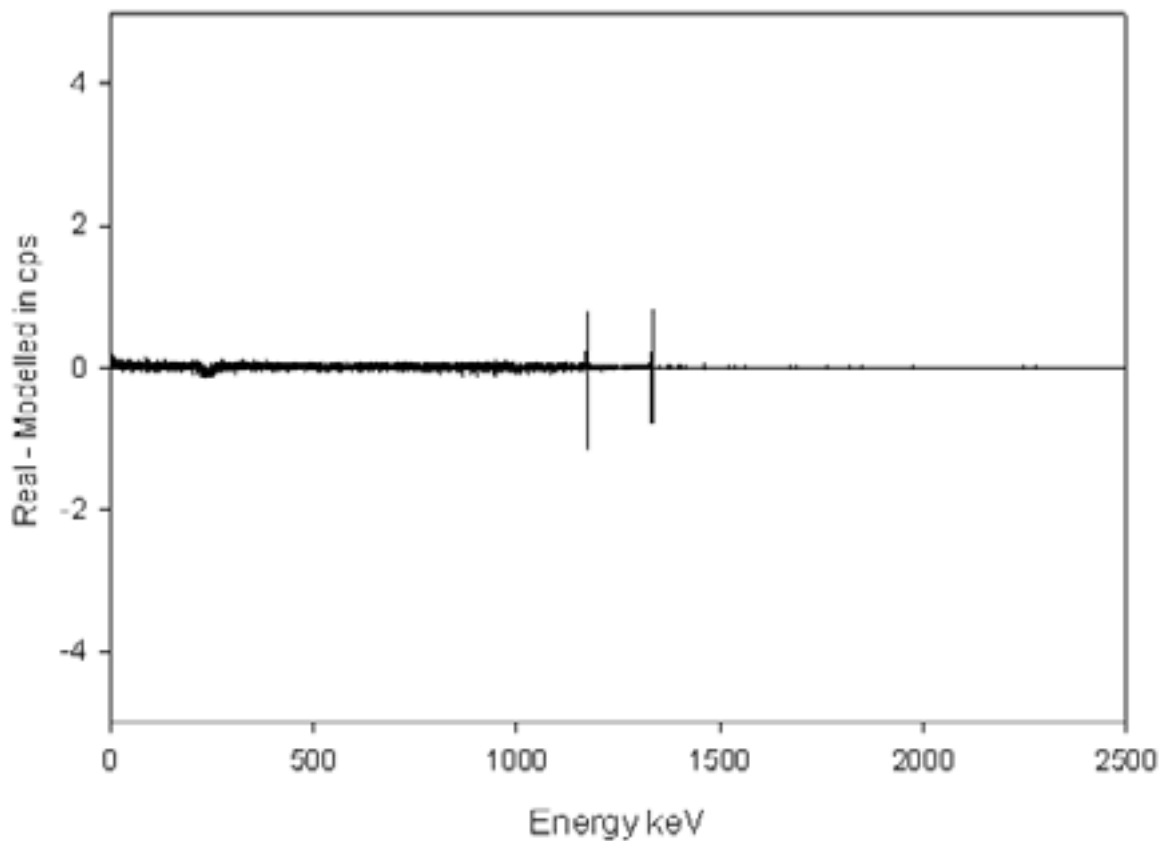


Figure 4.13 Difference between real and modeled ^{60}Co spectrum in counts per second per channel.

The ability to model spectra for various source – sample combinations is of some considerable use with respect to emergency preparedness activities. Currently, testing or development of analytical or response procedures with respect to high activity sources or sources consisting of nuclides that may not be part of the usually available suite is relatively complicated and not amenable to regular testing. Simulation of such sources and detectors responses to these sources constitutes a useful tool for both maintaining competence and developing new and effective response techniques with respect to both quantitative and qualitative methodologies. Outside of the arena of emergency response, simulation of detector response is a useful tool for optimizing analytical systems for regular monitoring activities or for establishing a systems ability to accurately and precisely measure nuclides which may not currently appear in the environment but could be introduced during release scenarios.

4.5. Total Coincidence Summation

Correction

Coincidence summing corrections were investigated for both ^{60}Co and ^{22}Na which are both vulnerable to the phenomenon. For point sources, spectra were simulated both with coincidence summing switched on and off and simulating the spectra with a resolution of 1 FWHM = 1 keV. The difference in the counts for the relevant peaks was used as the modeled correction factor. For the point sources, the deviation between the full energy peak efficiency curve as modeled by Monte Carlo and the empirically derived peak efficiency value was taken as the empirically derived coincidence correction factor.

For volumetric sources with ^{60}Co , the CSCOR program was used to determine the factors and these were compared with the factors determined for volumetric sources as for the

point sources. As can be seen in Table IX, good agreement was obtained for both isotopes at all energies for the different sources with respect to both empirically derived factors and those obtained with either the empirical method or the CSCOR program. It should be noted that when using an empirical procedure for the calculation of coincidence summation factors, the factor determined is vulnerable to the interpolation procedure used and therefore a degree of uncertainty is introduced as a result of the curve fitting.

The ability to determine coincidence correction factors constitutes a major advantage to using Monte Carlo based techniques. A wide range of isotopes are affected by the phenomenon and until recently correction for the problem was often ignored. As many laboratories strive to use monoenergetic sources for their calibration procedures and the number of isotopes visible in the environment that exhibit such summation is limited, many analysts are either unaware of the need for correction or do not know how to conduct it.

Because of a variety of factors, many laboratories may only first encounter isotopes needing significant correction during an accident scenario as was evidenced in the months after the Chernobyl accident when the problem resulted in widespread erroneous results for ^{134}Cs . It should also be noted that many natural nuclides encountered in monitoring programs exhibit complex decay schemes and concomitant coincidence summation that is often not accounted for in analysis results. Therefore any method that enables practicable exploration of the issue prior to situations such as that mentioned above is of considerable benefit.

Geometry	⁶⁰ Co 1173 keV		⁶⁰ Co 1332 keV		²² Na 1274 keV	
	Empirical	Modelled	Empirical	Modelled	Empirical	Modelled
15 mm	1.12+/-3%	1.093	1.11+/-3%	1.085	1.22	1.21
35 mm	1.04+/-3%	1.04	1.03+/-3%	1.034	1.13	1.13
55 mm	0.99+/-3%	1.02	1.0+/-3%	1.03	1.08	1.06
Geometry	CSCOR	Modelled	CSCOR	Modelled		
W1 10 mm	1.118	1.124	1.123	1.132		
W1 20 mm	1.098	1.108	1.103	1.114		
W2 10 mm	1.098	1.097	1.102	1.102		
W2 20 mm	1.084	1.087	1.088	1.092		

Table IX. Comparison of true coincidence summation correction factors derived by empirical methods and Monte Carlo simulation for ⁶⁰Co and ²²Na point sources and by CSCOR and Monte Carlo for ⁶⁰Co volumetric sources.

4.6. Implementation in Analysis Systems

The results of Monte Carlo simulation of detector efficiencies were implemented in two different gamma analysis systems. The first of these systems is an all inclusive system incorporating a range of correction features for the analysis of samples containing gamma emitting isotopes. In this system, fill height or geometry corrections are implemented independently of the efficiency data itself as are density corrections. Coincidence corrections are based on peak to total efficiency ratios and nuclear data contained within the library. For implementation of the Monte Carlo data in this system, two efficiency data sets were produced for the geometry in question at two different fill heights for an aqueous matrix of density 1. Once

obtained, these two sets are used internally by the software to produce a derivative efficiency data curve which serves as the primary efficiency data source for further analysis.

In the second system, possibly more typical of situations to be found in emergency situations removed from the laboratory, the system was only capable of producing spectral data and applying peak efficiency data towards the calculation of activities. No density, matrix or summation correction was implemented. In this case, Monte Carlo simulations were used to model the exact geometry and matrix which corrects for sample matrix or compositional corrections and simulations were run to determine summation correction factors for the

nuclides identified in the sample. These factors were then used to correct the nominal activity values to produce the final result. The sources used to test the implementation were two certified sources presented in the W2 geometry as described previously. The geometries contained either soil or simulated vegetation with densities of 1.6 and 0.45 respectively. The isotope suite chosen was a mixture of 6 isotopes presenting emissions in the energy range from 59 keV to over 1800 keV. Four of the isotopes featured cascade emissions requiring true coincidence correction, two of the isotopes also being vulnerable to the sample composition with

respect to deviations from a nominal aqueous calibration standard. The standards were chosen to represent a relatively complex sample requiring the full range of corrections to be applied. The samples were counted on the characterized detector T3 for a period sufficient to ensure 1 sigma uncertainties in the smallest photopeak of less than 5%. The spectra were then analyzed using both methods and the Monte Carlo data. The spectra were also analyzed using the inclusive software and an empirically derived calibration in daily use for gamma spectrometric analyses.

Isotope	Certified Activity Bq	Method1	Deviation	Method2	Deviation	Method 3	Deviation
¹³⁷ Cs	147.1+/-5	141.8+/-6	3.6	153.6+/-6	-4.4	152.2+/-18	-3.3
²⁴¹ Am	368.1+/-12	296.8+/-12	19.4	382+/-15	-3.8	375+/-24	-1.9
⁶⁰ Co	297.4+/-10	283.6+/-11	4.6	306.9+/-12	-3.2	301.6+/-20	-1.2
¹³⁴ Cs	399.9+/-13	388.7+/-16	2.8	412.6+/-17	-3.2	389.3+/-19	2.7
⁸⁸ Y	1230+/-41	1165+/-47	5.3	1244+/-50	-1.2	1235+/-65	-0.4
¹³³ Ba	240.6+/-8	215.5+/-9	10.4	225.6+/-9	6.2	240.2+/-14	0.2

Table X Comparison of certified activities for the test vegetation standard (density 0.6) with various analysis procedures: method 1 – inclusive software with empirical calibration data, method 2 – inclusive software with Monte Carlo derived calibration data, method 3 – regular spectral acquisition software with Monte Carlo derived calibration data and correction factors. Deviation refers to certified value minus determined value as percentage of certified value. Uncertainties given as 1 sigma in percent for methods, 2 sigma as percent for the certified standard.

Isotope	Certified Activity Bq	Method1	Deviation	Method2	Deviation	Method 3	Deviation
¹³⁷ Cs	147.1+/-5	151.5+/-7	-3.0	151+/-6	-2.7	155.2+/-5	-5.5
²⁴¹ Am	368.0+/-12	304.5+/-12	17.3	391+/-16	-6.3	384.2+/-6	-4.4
⁶⁰ Co	297.4+/-10	298.0+/-10	-0.2	295+/-12	0.8	311+/-6	-4.6
¹³⁴ Cs	399.8+/-13	407+/-14	-1.9	408.3+/-16	-2.1	387.6+/-5	3.1
⁸⁸ Y	1230+/-41	1219+/-37	1.0	1224+/-49	0.5	1260+/-6	-2.4
¹³³ Ba	240.6+/-8	234+/-7	2.7	251.1+/-10	-4.4	238.9+/-5	0.7

Table XI Comparison of certified activities for the test soil standard (density 1.6) with various analysis procedures: method 1 – inclusive software with empirical calibration data, method 2 – inclusive software with Monte Carlo derived calibration data, method 3 – regular spectral acquisition software with Monte Carlo derived calibration data and correction factors. Deviation refers to certified value minus determined value as percentage of certified value. Uncertainties given as 1 sigma in percent for methods, 2 sigma as percent for the certified standard.

Agreement between the methods was good as can be seen from Tables X and XI. Method 1 deploys a density correction method based on an aqueous matrix and seems in this case to have either overestimated the correction required for both the simulated vegetation and the soil sample or had an erroneous estimate of the efficiency at low energies to begin with. There appears to be a slight bias towards underestimation of the sources activities for the vegetation standard although is not replicated in the soil measurement. For the majority of the isotopes in both standards, the use of a Monte Carlo derived calibration appears to have reduced the deviation in most cases or produced a comparable value. Given that for Method 2 the original curve was produced by Monte Carlo for an aqueous geometry and corrections applied thereafter were as part of the analytical software, it may be that the disparities observed for Method 1 are most likely due to problems in the empirically derived efficiency curve of Method 1. It should also be noted that the emissions of ^{241}Am occur in a relatively difficult part of the spectrum and peak area determination can be affected significantly by this which may be contributing significantly to the deviations observed. Method 3 also produced quite good results for both standards. No evidence of a significant bias was observed for either standard and results obtained, even for complex isotopes such as ^{133}Ba are in agreement with those produced by the other methods. Method 3 modeled efficiency curves directly for the standard being used and coincidence factors were produced by simulation of the isotopes spectra with and without this phenomenon in geometries corresponding to the actual containers. From the results displayed it would appear that Monte Carlo routines are at least capable of producing results equivalent to those produced by more conventional methods with the added advantage of a suite of corrections being possible.

5. Conclusions

The results of the application of Monte Carlo methods to a number of aspects of relevance to gamma ray spectrometry indicate that the technique has a number of benefits to offer. Although unlikely to replace laboratory based conventional calibration methods for regular monitoring measurements, the methods confer a degree of flexibility and adaptability that is not present in conventional determinations of efficiency. This flexibility lends itself towards making measurements in emergency situations where access to a laboratory environment or its support facilities cannot be assured or in situations where speed of response is an issue.

In addition the methods provide a means of easily and efficiently solving a range of issues of concern in gamma ray spectrometry that would otherwise present difficulties. Of prominence among these are the problems associated with true coincidence summation or matrix corrections. Spectral simulation by itself is a significant tool in developing and maintaining analytical procedures and competence and constitutes a valuable means of simulating situations which require an efficient radioanalytical response but that may not have constituted a realistic threat 10 years ago.

Acknowledgements

The authors wish to acknowledge the staff of Bærum Hospital, Norway with respect to technical assistance and Dr Romano Plenteda of the Comprehensive Test Ban Treaty Organisation.

References

Abbas et al. 2001.

Abbas MI, Selim YS, Bassiouni M. HPGe detector photopeak efficiency calculation including self-absorption and coincidence corrections for cylindrical sources using compact analytical expressions. *Radiation Physics and Chemistry* 2001; 61: 429-431.

Atwater, 1972.

Atwater HF. Calculated total efficiencies of coaxial Ge(Li) detectors with small disc sources. *Nuclear Instruments and Methods* 1972; 104: 589-591.

Beattie and Byrne, 1972.

Beattie RJD, Byrne J. A Monte Carlo program for evaluating the response of a scintillation counter to monoenergetic gamma rays. *Nuclear Instruments and Methods* 1972; 104: 163-168.

Berger and Seltzer, 1972.

Berger MJ, Seltzer SM. Response functions for sodium iodide scintillation detectors. *Nuclear Instruments and Methods* 1972; 104: 317-332.

Bolivar et al, 1996.

Bolivar JP, Garcia-Tenorio R., Garcia-Leon M. A method for the determination of counting efficiencies in γ -spectrometric measurements with HPGe detectors. *Nuclear Instruments and Methods in Physics Research, Section A* 1996; 382: 495-502.

Chu et al, 1999.

Chu SYF, Ekström LP, Firestone RB. The LUND/LBNL nuclear data search. Version 2.0, February 1999. WWW table of radioactive isotopes.

<http://nucleardata.nuclear.lu.se/nucleardata/toi/>
∟ (01.08.06)

De Castro Faria and Levesque. 1967.

Castro Faria NV, Levesque R.J.A. Photopeak and double escape peak efficiencies of germanium lithium drift detectors. *Nuclear Instruments and Methods* 1967; 46: 325-332.

Debertin and Helmer, 1988.

Debertin K, Helmer RG. *Gamma- and x-ray spectrometry with semiconductor detectors*. Amsterdam: North-Holland, 1988.

Debertin and Jianping, 1989

Debertin K, Jianping R. Measurement of the activity of radioactive samples in Marinelli Beakers. *Nuclear Instruments and Methods in Physics Research, Section A* 1989; 278: 541-549.

Ford and Nelson, 1978.

Ford RL, Nelson WR. *The EGS code system: Computer programs for the Monte Carlo simulation of electron cascade showers (Version 3)*. SLAC-210. Stanford: Stanford University, 1978.

Fraczkiewicz and Walkowiak, 1992.

Fraczkiewicz R, Walkowiak W. Calculations of an effective solid angle including self-absorption correction applied to gamma-ray spectrometry analysis of natural samples. *Nuclear Instruments and Methods in Physics Research, Section B* 1992; 71: 434-540.

Freeman and Jenkin, 1966.

Freeman JM, Jenkin JG. The accurate measurement of relative efficiency of Ge(Li) gamma-ray detectors in the energy range 500 to 1500 KeV. *Nuclear Instruments and Methods* 1966; 43: 269-277.

Galloway, 1991.

Galloway R.B. Correction for sample self-absorption in activity determination by gamma spectrometry. *Nuclear Instruments and Methods in Physics Research, Section A* 1991; 300: 367-373.

Gilmore and Hemingway, 1996.

Gilmore G, Hemingway JD. *Practical gamma ray spectrometry*. New York: John Wiley and Sons, Inc., 1996.

Grosswendt and Waibel. 1975.

Grosswendt B, Waibel E. Determination of detector efficiencies for gamma ray energies up to 12 MeV - Monte Carlo calculation. *Nuclear Instruments and Methods* 1975; 131: 143-156.

Harvey, 1970.

Harvey JR. A formula for predicting the sensitivity of Ge(Li) spectrometers to gamma rays in the range 0.4–1.5 MeV. *Nuclear Instruments and Methods* 1970; 86: 89-197.

Heath, 1964.

Heath RL. *Scintillation spectrometry, gamma-ray spectrum catalogue*. 2nd Edition. Report IDO-16880. Idaho Falls: Idaho National Engineering Laboratory, 1964.

Helmer et al, 2004.

Helmer RJ, Nica N, Hardy JC, Iacob VE. Precise efficiency calibration of an HPGe detector up to 3.5 MeV, with measurements and Monte Carlo calculations. *Applied Radiation and Isotopes* 2004; 60: 173-177.

Hurtado et al, 2004.

Hurtado S, Garcia-Leon M, Garcia-Tenorio R. Monte Carlo simulation of the response of a germanium detector for low-level spectrometry

measurements using GEANT4. *Applied Radiation and Isotopes* 2004; 61: 139-143.

Knoll, 2000.

Knoll GF. *Radiation detection and measurements*. 3rd edition. New York: McGraw-Hill, 2000.

Korun and Martincic, 1992.

Korun, M, Martincic R. Efficiency calibration of gamma-ray spectrometers for volume-source geometry. *Applied Radiation and Isotopes* 1992; 43: 29 – 35.

Kushelevski and Alfassi, 1975.

Kushelevski AP, Alfassi ZB. Off center gamma ray detection efficiencies of cylindrical single open ended (SOE) Ge(Li) detectors. *Nuclear Instruments and Methods* 1975; 131: 93-95.

Lepy et al., 2001.

Lepy MC, Altitzoglou T, Arnold D et al. Intercomparison of efficiency transfer software for gamma-ray spectrometry. *Applied Radiation and Isotopes* 2001; 56: 71-75.

Moens et al. 1981.

Moens L, De Donder J, Lin XL et al. Calculation of the absolute peak efficiency of gamma-ray detectors for different counting geometries. *Nuclear Instruments and Methods* 1981; 187: 451-472.

Moens and Hoste, 1983.

Moens L, Hoste J. Calculation of the peak efficiency of high-purity germanium detectors. *Applied Radiation and Isotopes* 1983; 34: 1085-1095.

Plenteda, 2002.

Plenteda RA. Monte Carlo based virtual gamma spectroscopy laboratory. Vienna: Universitaetsbibliothek der Technischen Universitaet Wien, 2002.

Peterman et al, 1972.

Peterman BF, Hontzeas S, Rystephanick RG. Monte Carlo calculations of relative efficiencies of Ge(Li) detectors. Nuclear Instruments and Methods 1972; 104: 461-468.

Rogers, 1984.

Rogers DWO. Low energy transport with EGS. Nuclear Instruments and Methods, Section A 1984; 227: 535-548.

Sima and Arnold, 2000.

Sima O, Arnold D. Accurate computation of coincidence summing corrections in low level gamma-ray spectrometry. Applied Radiation and Isotopes 2000; 53: 51-56.

Sinkko and Aaltonen, 1985.

Sinkko K, Aaltonen H. Calculation of the true coincidence summing correction for different sample geometries in gamma-ray spectroscopy. STUK-B-VALO 40. Helsinki: Finnish Centre for Radiation and Nuclear Safety, STUK, 1985.

Somorjai, 1975.

Somorjai E. Note on the relation between efficiency and volume of Ge(Li) detectors. Nuclear Instruments and Methods 1975; 131: 557-558.

Sudarshan and Singh, 1991.

Sudarshan M, Singh, R. Applicability of the analytical functions and semi-empirical formulae to the full energy peak efficiency of large volume

HPGe gamma detectors. Journal of Physics D: Applied Physics 1991; 24: 1693-1701.

Tian et al, 2001.

Tian D, Xie D, Ho Y, Yang F. A new method to make gamma-ray self-absorption correction. Journal of Nuclear Science and Technology 2001; 38: 655-657.

Toufhanidis, 1983.

Toufhanidis N. Measurement and detection of radiation. New York: McGraw-Hill, 1983.

Vano, 1975.

Vano E, Gonzalez L, Gaeta R, Gonzalez JA. Relation between efficiency and volume of Ge(Li) detectors. Nuclear Instruments and Methods 1975; 123: 573-580.

Waino and Knoll, 1966.

Waino KM, Knoll GF. Calculated gamma ray response characteristics of semiconductor detectors. Nuclear Instruments and Methods 1966; 44: 213-223.

Weirkamp, 1963.

Weirkamp C. Monte Carlo calculation of photofractions and intrinsic efficiencies of cylindrical NaI(Tl) scintillation detector. Nuclear Instruments and Methods 1963; 23: 13-18.

Winn, 1993.

Winn WG. Evaluation of an exponential model for germanium detector efficiencies. Nuclear Technology 1993; 103: 262-273.

StrålevernRapport 2006:1
Virksomhetsplan 2006

StrålevernRapport 2006:2
Statens strålevern i Mammografiprogrammet. Resultater fra teknisk kvalitetskontroll hentet fra databaseprogrammet TKK

StrålevernRapport 2006:3
Avvikshåndtering ved norske stråleterapisentre

StrålevernRapport 2006:4
The Norwegian UV Monitoring Network 1995/96 - 2004

StrålevernRapport 2006:5
Sikkerhet ved russiske RBMK-reaktorer
En oppdatert gjennomgang av status

StrålevernRapport 2006:6
Radiologi i Noreg. Undersøkingsfrekvens per 2002, tidstrender, geografisk variasjon og befolkningsdose

StrålevernRapport 2006:7
Tiltak mot radon i privatboliger
Oppsummering av tiltak under Nasjonal kreftplan 1999-2003

StrålevernRapport 2006:8
K-159. Havariet av den russiske atombåten K-159 og den norske atomberedskapsorganisasjonens håndtering av ulykken